Minimizing residual black particles in sand filtrate when applying super-fine powdered activated carbon: coagulants and coagulation conditions

Yoshifumi Nakazawa [a], Yoshihiko Matsui [b*], Yusuke Hanamura [a], Koki Shinno [a], Nobutaka Shirasaki [b], and Taku Matsushita [b]

a Graduate School of Engineering, Hokkaido University, N13W8, Sapporo 060-8628, Japan

b Faculty of Engineering, Hokkaido University, N13W8, Sapporo 060-8628, Japan

* Corresponding author. Tel./fax: +81-11-706-7280

E-mail address: matsui@eng.hokudai.ac.jp

Abstract

Because of the eminent adsorptive capacity and rate for dissolved organic molecules compared to conventionally-sized powdered activated carbon (PAC), super-fine powdered activated carbon (SPAC) is gathering momentum for use in not only the pretreatment for membrane filtration for drinking water purification but also the conventional water purification process consisting of coagulation-flocculation, sedimentation, and rapid sand-filtration (CSF). However, the probability of SPAC particles to leak through a sand bed is higher than that of PAC, and their strict leakage control is an issue to be challenged when applying SPAC to CSF. However, study focusing on very high particle removal, which yield residual concentrations down to around 100 particles/mL, has been very limited. A previous study mentioned that the tendency of SPAC leakage is related to its low destabilization. In response to this, the present study focused on the two key components of coagulation (mixing intensity and coagulants) and investigated how to effectively reduce the residual SPAC after CSF.

Astonishingly, the flash mixing (the first process of CSF), especially its G (velocity gradient) value, played the most important role in determining the residual SPAC in the filtrate of sand filter (the fourth process). Even if the slow mixing time was short, a sufficiently large G value but short T (mixing time) value in flash mixing effectively reduced the residual SPAC. When the total GT value of flash and slow mixing was fixed at a constant, priority should be given to flash mixing to reduce the residual SPAC.

Among 23 PACl (poly-aluminum chloride) coagulants, PACl with a high-basicity (basicity 70%) and with sulfate ion (0.14 of sulfate/aluminum in molar ratio), produced by $Al(OH)_3$-dissolution, were the most effective to reduce the residual SPAC after CSF. PACls produced by base-titration, which have been intensively investigated in previous researches, were not effective due to lack of floc-formation ability. However, their Al species composition

43 determined by the ferron method were almost the same as those of PACl by $Al(OH)_3$-
44 dissolution, and their charge-neutralization capacities were higher. PACls produced by
45 $Al(OH)_3$-dissolution possessed both charge-neutralization and floc-formation abilities, but
46 the former ability was more important to minimize the residual of SPAC.
47
48
49 **Keywords**
50 SPAC; filtration; mixing; floc; basicity
51

1. Introduction

When removing dissolved organic compounds, in particular those of low molecular size, in water treatment processes, adsorption by activated carbon (AC) has been a common practice for many years. Activated carbon is used as an adsorbent either in powdered or granular form. While granular activated carbon is used in a bed adsorber, powdered activated carbon (PAC) can be applied at any point in the treatment process if PAC is sufficiently removed before the treated water enters the distribution system. The main concern for the adsorption processes is the removal efficiencies of target adsorbate compounds to be treated, but plant operators also pay attention to avoid fine black carbon particles from remaining in treated water and entering the distribution system. It is actually not uncommon that PAC, which is applied upstream of a separation process such as rapid sand filtration, sometimes passes through the filters and enters the distribution system, provoking black or grey water complaints from consumers (American Society of Civil Engineers and American Water Works Association 1998). Black water is usually caused by inadequate coagulation and sedimentation or high doses of PAC (American Water Works Association and American Society of Civil Engineers 2012). Even trace concentrations of black carbon particles remaining in treated water, which do not make the water black or grey and do not violate drinking water quality standards for turbidity, could deteriorate the quality of food, such as tofu, that is produced from the water, etc., which causes complains from food manufacturers. Plant operators pay closer attention to the turbidity or particle count in treated water when PAC is dosed than when PAC is not dosed (Bureau of Waterworks Tokyo Metropolitan Government 2014). Control of fine, black carbon remaining in treated water should be a critical issue, in particular, under the situation in which the application of super-fine PAC (SPAC), carbon particles with a size smaller than

76 the conventional size, attracts attention (Amaral et al. 2016, Ando et al. 2010, Bonvin et al.
77 2016, Ellerie et al. 2013, Matsui et al. 2004, Matsui et al. 2012, Partlan et al. 2016).
78
79 Plenty of studies have been conducted for the effect of coagulants and coagulation conditions
80 on floc formation and turbidly removal (Letterman and Yiacoumi 2011). Some studies have
81 been conducted for the effect of PAC on coagulation-sedimentation; however, studies
82 regarding the control of carbon particles at trace concentration levels are very limited. Aguilar
83 et al. (2003) reported that the use of PAC considerably increased the elimination efficiency
84 of particulate matters by coagulation and sedimentation, but there was a diminution in the
85 elimination efficiency for particles with diameters in the range 5.5–8.5 μm. They attributed
86 this diminution to the carbon particles remaining in the treated water. In contrast, Younker
87 and Walsh (2016) reported that the addition of PAC into $FeCl_3$ flocs reduced floc size but
88 had little impact on final turbidity after sedimentation. Therefore, the researches of the two
89 reports are not completely consistent with regard to the effect of PAC, but several reasons
90 can be considered for this apparent discrepancy: raw water characteristics, coagulation
91 conditions employed, etc. The effects of SPAC and PAC on floc formation were investigated
92 in a membrane filtration study (Matsui et al. 2009). The authors reported that the floc particles
93 that formed during coagulation preceded by SPAC pretreatment were larger and more porous
94 than the floc particles formed during coagulation preceded by PAC pretreatment and those
95 formed during coagulation without any pretreatment. The authors explained this result due
96 to increased particle–particle collision frequency and better removal of natural organic
97 matter, which inhibits coagulation by consuming coagulant, before the coagulation reaction.
98 These previous researches focused on the effect of adsorbent on the formation of floc
99 properties, settling velocity, permeability etc., and carbon particles have been investigated as

100 a ballasting agent for settling, nuclei for coagulation, or a pretreatment agent of coagulation-
101 hindering compounds.
102
103 However, researches to investigate the effect of coagulation conditions and coagulants on the
104 remaining carbon particles in finished water have, to the best of our knowledge, never been
105 conducted except for that of our research group, although their control at a trace concentration
106 level is an important issue in terms of customer satisfaction. Our research group recently
107 revealed that at equivalent carbon doses to achieve the same adsorptive removal performance
108 (30 mg/L for PAC and 7.5 mg/L for SPAC), the residual particle number concentrations after
109 coagulation-flocculation, sedimentation, and sand filtration (CSF) were similarly low (100–
110 200 particles/mL) between SPAC and PAC and the particle sizes were similarly small
111 (Nakazawa et al. 2018). There is no drinking water quality standard or guideline in the world
112 for black carbon particles, to the best of our knowledge. When applying SPAC instead of
113 PAC, however, a criterion from plant operator sites, in particular those with a safety
114 orientation, would be that the level of carbon particles remaining in treated water when SPAC
115 is applied should be at a similar or lower level than when PAC is applied.
116
117 On the basis of these consideration, this study set its objectives to find better coagulation
118 conditions and find a better coagulant (poly-aluminum chloride: PACl) for the removal of
119 SPAC. In actual water treatments, SPAC/PAC is applied for the removal of dissolved organic
120 compounds, and the removal of SPAC/PAC by CSF occurs in the presence of other
121 substances, such as clay particles and natural organic matter, which may influence the
122 removal of SPAC/PAC. Moreover, coagulation conditions better for SPAC removal may
123 necessarily not bring a good performance for natural organic matter removal. However, the

CSF experiments in this study were conducted mainly with water made from filtered tap water supplemented with carbon slurry in order to gain basic information for carbon particle removal without any influence of other substances.

2. Materials and Methods

2.1. *Activated carbon particles*

A commercially available wood-based PAC (Taiko W; Futamura Chemical Co., Ltd., Nagoya, Japan) was prepared as a slurry in pure water (Milli-Q water; Merck KGaA, Darmstadt, Germany) at a concentration of ~15% (w/w). The PAC in the slurry were milled in a closed-chamber ball mill (Nikkato, Osaka, Japan) with 5- and 10-mm-diameter Al_2O_3 balls at 45-50 rpm for 4–5 h to afford the particles with D_{95} (the diameter larger than 95% of the entire distribution) < 30 μm (Pan et al. 2017). The slurry was taken out from the chamber of the ball mill and then milled with a bead mill (LMZ015, Ashizawa Finetech, Ltd., Chiba, Japan) with 0.3-mm-diameter ZrO_2 beads at a rotational speed of 8 m/s (2590 rpm) in recirculation mode for 20 min to produce a SPAC slurry (Table 1).

The true particle size distributions of the carbons were determined using a laser light diffraction and scattering method (Microtrac MT3300EXII, Nikkiso Co., Inc., Tokyo, Japan), which followed addition of a dispersant (Triton X-100; Kanto Chemical Co., Inc., Tokyo, Japan; final concentration, 0.08% w/v) and ultrasonic dispersion with 150 W for 1 min (Fig. 1S, Supplementary Information of SI).

140 2.2. *Coagulants*

141

142 Twenty-three kinds of PACls were used as coagulants in the present study. Among them,
143 PACl-70 (basicity 2.1; the number, 70, in the name indicates the % basicity; sulfate ion 2%
144 w/w) and PACl-50 (basicity 1.5, sulfate ion 3% w/w) are commercial products provided by
145 Taki Chemical Co., Ltd. (Hyogo, Japan), which are produced by dissolving $Al(OH)_3$ into
146 HCl and H_2SO_4 [as described by, e.g., Itoh and Sato (1995) and Sato and Matsuda (2009)].
147 On the other hand, B70ns, B70s0.11, B70s0.12, B70s0.13, B70s0.14, B70s0.15, and
148 B70s0.17 (the numbers after "B" and "s" represent the "% basicity" and "mole ratio of sulfate
149 ion to aluminum: SO_4/Al" respectively, and "ns" stands for "non-sulfated") were produced
150 in the authors' laboratory by the following method named $Al(OH)_3$-dissolution.

151

152 Predetermined amounts of $AlCl_3 \cdot 6H_2O$ (FUJIFILM Wako Pure Chemical Corporation,
153 Osaka, Japan) and $Al_2(SO_4)_3 \cdot 14\sim18H_2O$ (FUJIFILM Wako Pure Chemical Corporation)
154 were dissolved into pure water (Milli-Q water) to get aluminum aqueous solution. This
155 solution was mixed with $Al(OH)_3$ powder (FUJIFILM Wako Pure Chemical Corporation) to
156 form a milk-like slurry and then heated with microwaves (ETHOS TC, Milestone S.r.l.,
157 Sorisole (BG), Italy) at 150°C for 3 h. After that, the slurry was centrifuged by a centrifugal
158 separator (H-9R, Kokusan Co., Ltd., Tokyo, Japan) at a rotation speed of 3,000 rpm (6,000
159 g) for 10 min at 20°C, and then the clear top of the liquid was filtered by a membrane filter
160 (pore size 0.45 μm, PTFE, Toyo Roshi Kaisha, Ltd., Tokyo, Japan) to obtain a solution of
161 PACl with basicity of 40~50%. The solution was poured into a beaker, stirred with a rotation
162 speed of >600 rpm, and heated at 50°C using a hot plate/magnetic stirrer, and then a
163 predetermined amount of aqueous solution of sodium carbonate (FUJIFILM Wako Pure

Chemical Corporation) was dripped into the solution to adjust the basicity up to 70%. The basicity was calculated by the following formula.

$$\text{Basicity (\%)} = \frac{[OH^-]}{3[Al_t]} \times 100$$

where $[Al_t]$ is the total aluminum concentration determined by an inductively coupled plasma mass spectrometer (ICPMS, 7700x, Agilent Technologies, Inc., Santa Clara, CA, USA), $[OH^-]$ is the concentration of hydroxyl groups from the ingredients $Al(OH)_3$ and sodium carbonate. The total mass of OH^- introduced to the final product was calculated by taking a mass balance.

PACls produced by the method named base-titration were used in the CSF experiments described in supplementary experiments. The method is described in SI.

The distributions of aluminum species in the coagulants were analyzed by the ferron method. On the basis of their reaction rates with ferron reagent (8-hydroxy-7-iodo-5-quinoline sulfonic acid, FUJIFILM Wako Pure Chemical Corporation), the aluminum species were divided into three categories: Ala, Alb, and Alc. Ala denotes aluminum species that reacted with ferron instantaneously (within 30 s). Alb denotes species that reacted with ferron within 120 min. Alc denotes species that did not react with ferron. These species were assumed to be monomeric, polymeric, and colloidal aluminum species, respectively (Wang et al. 2004). Ferron analyses of the PACls were conducted immediately after dilution with Milli-Q water to 2.7 g-Al/L (0.1 mol-Al/L) (Jia et al. 2004, Wang et al. 2004). Dilution reportedly has little effect on the ferron speciation distribution of PACl (Kimura et al. 2013, Wang et al. 2002).

188

189 2.3. *Coagulation–flocculation, sedimentation, and rapid sand filtration*

190

191 Tap water in Sapporo city was filtered through a membrane filter (nominal pore diameter,
192 0.1 μm; Toyo Roshi Kaisha, Ltd.) to remove suspended matter, and then the water was
193 adjusted for M alkalinity to 30 mg/L as $CaCO_3$ by adding $NaHCO_3$ (FUJIFILM Wako Pure
194 Chemical Corporation). The water was supplemented with an activated carbon slurry to make
195 a raw water for CSF experiments: activated carbon concentrations were 30 mg/L for PAC; 6
196 mg/L, 7.5 mg/L, 10 mg/L, or 30 mg/L for SPAC. Most CSF experiments were conducted
197 with these waters, but some CSF experiments were additionally conducted with water from
198 the Toyohira River (Sapporo, Japan) after supplementing it with SPAC at 10 mg/L. The river
199 water was sampled at the location where it becomes the raw water source for the Moiwa
200 Water Purification Plant (Sapporo).

201

202 The experimental setup and procedure were basically the same as those of Nakazawa et al.
203 (2018) but are shown in Fig. 2S (SI). The coagulation–flocculation and sedimentation steps
204 were conducted in a 4-L rectangular beaker. After a predetermined volume of HCl or NaOH
205 (0.1 N) was added to adjust the coagulation pH to 7.0, the coagulant (PACl) was injected into
206 the beaker to a final concentration of 4 mg-Al/L, unless otherwise noted. Then the water was
207 mixed rapidly followed by slow mixing with a three-stage mixing intensity. The mixing
208 intensities (G value: velocity gradient, see Fig. 3S and Table 1S of SI for the G value
209 calculation) and times (T value: mixing time) of the flash (indicated by subscript F) and slow
210 mixing (indicated by subscript S, with the order: 1, 2, and 3) were varied depending on each
211 experiment, and these values are described in each case in the Results and Discussion section

212 (see also Table 2S, SI). The water was then left at rest for 1 h. Next, the top three liters of the
213 water (supernatant) were transferred to another beaker for determination of the turbidity
214 (2100Q portable turbidimeter; Hach Company, Loveland, CO, USA) and for rapid sand
215 filtration. Sand filtration was conducted for 40 min at a rate of 90 m d^{-1} in the down-flow
216 direction using a column (Φ4 cm) filled to a depth of 50 cm with sand (effective diameter,
217 0.6 mm; uniformity, 1.3). The sand filtrate was collected from 13 to 40 min after the start of
218 filtration, and the turbidity and carbon particle count of the filtrate were determined. After
219 each filtration run, the sand filter was backwashed with tap water, then washed forward with
220 pure water (Milli-Q water) and membrane-filtered tap water.
221
222 *2.4. Membrane filtration and microscopic image analysis*
223
224 To sample the carbon particles in the water, the water was filtered through a PTFE membrane
225 filter (nominal pore diameter, 0.1 μm; Φ25 mm; Merck KGaA) supported by a glass filter
226 holder (KG-25; Toyo Roshi Kaisha, Ltd.) (Fig. 4S, SI). After drying the filter, color digital
227 photomicrographs were captured for nine or eighteen predetermined observation zones
228 (microscope view area, 247×330 μm) per filter (Fig. 5S, SI) with a digital microscope (VHX-
229 2000; Keyence corporation, Osaka, Japan) at 1000× magnification. The photomicrographs
230 were analyzed using the image analysis software supplied with the microscope. Details of
231 the analytical procedures are reported elsewhere (Nakazawa et al. 2018).
232
233
234 **3. Results and Discussion**
235

236 *3.1. Comparison of commercially-available PACl-50 and PACl-70*

237

238 Fig. 1 shows the number concentrations of residual carbon particles in sand filtrate after CSF
239 when water containing SPAC or PAC of various mass concentrations was coagulated using
240 PACl-70 (a high-basicity PACl) or PACl-50 (a conventional PACl having normal basicity).
241 When PAC at the initial concentration 30 mg/L was treated with PACl-70, the residual
242 concentrations were around 200 particles/mL, and PACl-70 resulted in a slightly higher
243 residual concentration than PACl-50, but the difference was small.

244

245 When SPAC of the same initial concentration (30 mg/L) was treated using conventional
246 PACl-50, the residual concentration was much higher (800 particles/mL). When PACl-70
247 was used to treat the SPAC, the residual concentration was reduced to 400 particles/mL. The
248 lower the initial concentration of SPAC was, the lower the residual concentration, both for
249 PACl-50 and PACl-70; and at the initial concentration of 7.5 mg/L or less, the difference of
250 residual concentrations between the two cases of using PACl-50 or PACl-70 became smaller.
251 Overall, high-basicity PACl-70 was superior to PACl-50 to remove SPAC. With PACl-70,
252 the removal rates in terms of particle number concentrations depended on the concentration
253 of SPAC: 5.3 log removal was lowest at an SPAC concentration of 10 mg/L. Nevertheless,
254 the removal rates with PACl-70 were slightly higher than with PACl-50 (Fig. 6S, SI). In
255 contrast, the turbidity of the supernatant after sedimentation following coagulation by PACl-
256 50 was slightly lower than that by PACl-70, and the result was opposite to the residual
257 number concentration mentioned above (Fig. 7S, SI).

258

259 Higher-basicity PACls (e.g. PACl-70) are known to neutralize negative charges more
260 according to the results of colloid titration (Fig. 8S, SI) (Matsui et al. 2017). Accordingly,

261 although PACl-70 is not superior compared with PACl-50 in terms of forming large flocs
262 bringing a lower turbidity of supernatant water, PACl-70 is inferred to neutralize the negative
263 charges of carbon particles efficiently due to its high capacity in charge neutralization. The
264 high capacity in charge neutralization seemed to contribute to the removal of carbon particles.
265
266 We previously reported that the particles remaining after CSF were smaller in size than the
267 particles before CSF (Nakazawa et al. 2018). Although the tendency of small carbon particles
268 to remain after CSF is overall attributable to their size, the size effect is comprised of the
269 following three reasons: 1) low destabilization rate during the coagulation process, 2) low
270 frequency of particle–particle collisions during flocculation, and 3) low probability of the
271 particles coming into contact with sand grains during the sand filtration process. Therefore,
272 particle destabilization is a key to reduce remaining carbon particles after CSF. When
273 comparing the zeta potentials of residual carbon particles after CSF treatments with PACl-
274 70 and PACl-50, they were not different (Fig. 2). Therefore, particles with a certain zeta
275 potential value or lower regardless of PACl-70 or 50 passed through the filter. Accordingly,
276 the merit of PACl-70 in reducing carbon particle concentration after CSF was due to its high
277 capacity to minimize the number of non-neutralized carbon particles (with a certain zeta
278 potential value or lower) rather than due to its high positive charge to neutralize the negative
279 charge of particles to nearly zero level.
280
281 When the SPAC suspension was coagulated using PACl-70, the formation of micro floc
282 particles was not confirmed in the photograph taken soon after flash mixing (Fig. 3). When
283 the PAC suspension was coagulated with PACl-70, the formation of micro floc particles was
284 confirmed marginally. In contrast, when PACl-50 was used in the coagulation process, the
285 formation of micro floc particles was clearly observed in the experiments of all experimental

conditions. However, floc size at the end of slow mixing was not different between each pair of experiments using PACl-50 and PACl-70.

Therefore, it can be said that the rapid formation of large-size floc particles and the lowered turbidity of supernatant water, although such information can be obtained by a conventional jar test, are not indicators for a lower residual carbon particle concentration after CSF. PACls are rich in diversity in terms of two different aspects: charge-neutralization capacity to destabilize particles and the bridge-formation ability to form large floc particles, but the charge-neutralization capacity is not related to the bridge-formation ability (Zhao et al. 2010). Consequently our study revealed that PACls having a feature of the charge-neutralization capacity to destabilize particles rather than the bridge-formation ability to form large-size floc particles are beneficial for lowering residual carbon particle concentration after CSF.

3.2. Effect of mixing intensity in coagulation and flocculation

As mentioned in the preceding paragraph, the high-basicity PACl (PACl-70) formed flocs slowly, but it had a high charge neutralizing capacity. Hence, it was hypothesized that optimizing the mixing intensity and time would lead to further reduction of residual carbon particle concentration in sand filtrate, and experiments were conducted. Fig. 4 illustrates the residual SPAC concentrations in sand filtrates when coagulation-flocculation were conducted with three different G_TT_T values ranging from 19,500 to 78,000 by adjusting T_T. (The G_TT_T value means total GT, which is the sum of flash-mixing GT (G_FT_F) and slow-mixing GT (G_ST_S).) In the case with the small G_TT_T value of 19,500, the residual carbon particle concentration was 800-particles/mL after CSF using PACl-50, whereas a much higher residual concentration of 2,200 particles/mL was observed using PACl-70. In such a low

311 mixing intensity, large floc particles were seen in the photographs at the end of slow mixing,
312 but many small floc particles were also observed in the same photographs, in both cases of
313 PACl-50 and PACl-70 (Fig. 5); the mixing intensity was obviously insufficient. In contrast,
314 as the G_TT_T value increased from 39,000 to 78,000, small floc particles diminished, seen in
315 the photographs taken at the end of slow mixing (Fig. 5). At the same time, the turbidity of
316 supernatant water (Fig. 9S, SI) and the residual carbon particle concentration of sand filtrate
317 also decreased substantially. As shown in Fig. 4 and Fig. 9S (SI), furthermore, the effect of
318 G_TT_T on the turbidity of supernatant water and the residual carbon particle concentration of
319 sand filtrate was more pronounced for PACl-70, which had a higher capacity for charge
320 neutralization, than PACl-50.
321
322 *3.3. Effect of flash mixing intensity in coagulation*
323
324 Because charge neutralization occurs mostly during the flash mixing stage, we hypothesized
325 that the residual carbon particle concentration of sand filtrate is influenced more by the flash
326 mixing conditions than by the slow mixing conditions, so we conducted other series of CSF
327 experiments. In the first series of experiments, the G_TT_T was fixed at 39,000, but its allocation
328 to flash mixing was changed; i.e. the larger the G_FT_F value of flash-mixing was, the smaller
329 the G_ST_S value of slow-mixing. The results are shown in Fig. 6. When the flash-mixing G_FT_F
330 was small (6,000), the residual carbon particle concentration was high at 900 particles/mL.
331 The residual concentration, however, decreased as the flash-mixing G_FT_F increased. The
332 effect of the flash-mixing G_FT_F was more prominent with PACl-70 than with PACl-50. At
333 the largest flash-mixing G_FT_F (24,000), the residual carbon particle concentration was
334 reduced to <200 particles/mL.
335

336 In a series of experiments for which flash-mixing G_FT_F was changed by adjusting T_F but slow
337 mixing intensity was fixed at a constant value (G_ST_S=15,100), a G_FT_F >24,000 resulted in a
338 low residual carbon particle concentration (Fig. 7), indicating that there is a certain minimal
339 value for G_FT_F required for lowering the carbon particle concentration in sand filtrate. Next,
340 the effect of G_F value on residual carbon particles was examined in the condition where GT
341 values of both flash and slow mixing intensities were fixed (G_FT_F=24,000 and G_ST_S=15,100).
342 Residual carbon particle concentration became smaller with a larger G_F value (smaller T_F
343 value) (Fig. 8). It was minimal at G_F=600 s^{-1} (experiments at G value>600 s^{-1} could not be
344 conducted because the mixing caused the water to splash out of the container. Kan et al.
345 (2002) conducted jar tests by using alum and commercially-available PACl to investigate the
346 effect of flash-mixing time on the removal of clay particle. They report that the residual
347 turbidity decreased sharply with increasing duration of flash-mixing. Lin et al. (2013) also
348 conducted jar tests by using turbid surface-water and commercially-available PACl to
349 investigate the effect of flash-mixing intensity on the turbidity and DOC removal. They
350 reported that the removal performances of turbidity and DOC were improved as flash-mixing
351 intensity increased. We used fine carbon particles as the target matter in the present study,
352 but the tendency that the turbidity after settling and residual carbon particles remaining in
353 sand filtrate reduced as flash-mixing intensity or time increased was much the same as those
354 previous studies.
355
356 It is of great interest that the trace residual-carbon-particle concentration as an outcome after
357 the fourth step of sand-filtration in the CSF was largely affected by the mixing intensity of
358 the first step of coagulation in the CSF, although the flocculation and sedimentation processes
359 occurred in between the coagulation and the sand-filtration. The flocculation and
360 sedimentation processes had long detention time, and most of the carbon particles were

361 removed by the sedimentation process. During the flash mixing process for coagulation, the
362 PACls hydrolyzed in water and formed a hydrolyzing aluminum polymer, which efficiently
363 neutralized the negative charge of carbon particles. Thus, providing both rapid dispersion of
364 dosed PACls and high-frequent contact between the hydrolyzing aluminum polymer and the
365 carbon particles, in particular very fine carbon particles, was necessary to decrease charge-
366 un-neutralized particles. Finally, achieving these conditions produced low residual carbon
367 particles, which penetrated through the sand bed situated in the last stage in the CSF. A high
368 G_F value created such conditions of the rapid dispersion and the high-frequent contact.
369
370 *3.4. Effect of coagulant dosage*
371
372 It is generally known that turbidity removal by coagulation-sedimentation improves as the
373 dosage of coagulant increases when the coagulation processes are mainly due to sweep
374 flocculation mechanism, which operates at near neutral pH, but not due to charge-
375 neutralization mechanism, which operates at pH < 6 (Amirtharaja and O'Melia 1990,
376 Hendricks 2010, Letterman and Yiacoumi 2011). The present study of CSF, which was
377 conducted at pH 7, also confirmed the relationship between the dosage of coagulant and the
378 residual concentration of SPAC or the turbidity of supernatant water in CSF (Fig. 10S and
379 Fig. 11S, SI); increasing coagulant dosage resulted in an increase in the removal of carbon
380 particles both after sedimentation and sand filtration. Additionally, the superiority of PACl-
381 70 to PACl-50 was held in the entire range of coagulant dosages tested in terms of residual
382 carbon particle concentration. The very low residual concentration of 6 particles/mL was
383 attained with the highest coagulant dosage of PACl-70.
384
385 *3.5. Development and performance of coagulants by base-titration*

386

387 The above described investigation suggests the importance of decreasing the number of
388 charge-un-neutralized particles in order to enhance the separation of SPAC particles and
389 lower the number of residual SPAC particles after CSF. Available techniques for decreasing
390 the number of charge-un-neutralized particles were enumerated using a coagulant with high
391 a charge-neutralization capacity, such as high-basicity PACl with the optimized flash mixing
392 intensity, as well as increasing the dosage of coagulant. We further searched for a better PACl
393 that lowered the number of residual SPAC particles. We produced a series of PACls with
394 high basicity (Table 3S, SI) and conducted jar tests (Table 4S, SI).
395

396 It is widely known that the Al_{13} species in PACl have a high charge-neutralizing ability (Gao
397 et al. 2005, Lin et al. 2008, Parthasarathy and Buffle 1985, Wu et al. 2007, Zhao et al. 2009),
398 and Alb analyzed by the ferron method corresponds to the Al_{13} species (Parker and Bertsch
399 1992, Parthasarathy and Buffle 1985). In the present study, some PACls with a high content
400 of Alb (Alb-type PACl) were produced by base-titration (Fig. 12S, SI), and experiments of
401 coagulation-flocculation and sedimentation were conducted. The zeta potential of carbon
402 particles became zero at a lower dosage of Alb-type PACl (B80ns-1) than of PACl-70 (Fig.
403 13S, SI), and Alb-type PACls (B65ns, B80ns-1, B80ns-2) supplied a higher positive charge
404 to carbon particles than PACl-70 at the same coagulant dosage (Fig. 14S, SI). These results
405 indicate that Alb-type PACls actually had a higher charge-neutralizing ability than PACl-70.
406 However, these Alb-type PACls could not flocculate carbon particles, and consequently
407 resulted in a high turbidity after sedimentation, even given large mixing intensity (Fig. 14S,
408 SI). Even at the coagulant dose, which brought the zeta potentials of carbon particles to
409 around zero, the turbidities after sedimentation were still high, compared with those obtained
410 by PACl-70 (Fig. 13S, SI).

411

412 It was reported that sulfate ions in PACl play a role in enhancing floc formation (Wang et al.
413 2002). Actually, the commercial PACl products, PACl-50 and PACl-70, both of which
414 produce larger floc particles than the Alb-type PACl, contain sulfate ion. Accordingly, we
415 supplemented sulfate ion and prepared three Alb-type PACls (Fig. 15S, SI). One PACl
416 (B82s0.11) among the sulfated Alb-type PACls slightly flocculated carbon particles at a large
417 mixing intensity (as a GT value of 57,000). However, turbidity-removal performance was
418 considerably inferior to PACl-50 and PACl-70.

419

420 Gao and Yue (2005) produced sulfated PACls of different SO_4/Al ratios by base-titration at
421 ambient temperature and reported that a sulfated high-basicity PACl (basicity 67%) with
422 SO_4/Al=0.066 in the range from 0 to 0.15 reduced residual turbidity the most when an
423 experiment consisting of coagulation-flocculation and sedimentation was conducted with
424 lake water. In our experiments, however, the production of sulfated high-basicity PACls at
425 ambient temperature by base-titration was unsuccessful due to the occurrence of aluminum
426 hydroxide precipitation during titration, and we were not able to apply the sulfated high-
427 basicity PACl. Shi et al. (2007) also mentioned that room temperature was not suitable for
428 preparation of PACl because a large amount of aluminum precipitate could form during
429 titration.

430

431 Yan et al. (2008) investigated the relationship between Al species and their behavior in
432 coagulation targeting NOM. They reported that Ala (monomeric species) combined with
433 NOM but most of the flocs formed by Ala were small and difficult to settle. Alb (polymeric
434 species) had high charge-neutralizing ability but flocs formed by Alb were not larger and did
435 not settle faster than those formed by Alc (colloidal species), and Alc adsorbs and removes

436 the target matter most efficiently. In the present study, in addition, given that the major
437 aluminum fraction in PACl-50 and PACl-70 was not Alb but Alc, Alc-type PACls (rich in
438 content of Alc fraction) were also produced (see SI for the preparation method). Those Alc-
439 type PACls showed high charge-neutralization ability, however their flocculation
440 performances were almost the same as the Alb-type PACls and had a low removal efficiency
441 (Fig. 16S, SI). In summary, Alb or Alc in PACls prepared by base-titration had a high
442 capacity for charge-neutralization, but the bridge-formation ability to form floc particles was
443 poor and resulted in high turbidity after sedimentation.
444
445 *3.6. Development and performance of coagulants by $Al(OH)_3$-dissolution*
446
447 Subsequently, we applied another method to produce PACls: $Al(OH)_3$-dissolution (Table 2).
448 Eleven PACls with a basicity of 70% and with a variety of sulfate ion contents were produced
449 (Table 2): it was impossible to produce PACls with a basicity >70% because of the gelation
450 of Al solution or the presence of too much undissolved residue. As shown in Fig. 9, the
451 performance on reducing residual SPAC particles increased as sulfate content increased from
452 $SO_4/Al=0$ to $SO_4/Al=0.14$ but decreased for $SO_4/Al>0.14$. The preparation of PACls with
453 $SO_4/Al>0.14$ required rising the temperature from 50°C to 80°C when adjusting the basicity.
454 In terms of high temperature, this process was similar to the process of base-titration PACls,
455 which do not have sufficient bridge-formation ability. The loss of the bridge-formation ability
456 might be related with a high temperature in production process.
457
458 Among the PACls prepared by $Al(OH)_3$-dissolution, B70s0.14 with the $SO_4/Al=0.14$ showed
459 the highest performance on reducing residual SPAC particles after CSF. B70s0.14

460 outperformed commercially available PACl-70, which was used in the experiments of the
461 paragraph 3.1, 3.2, and 3.3 and effectively removed SPAC. As shown in Fig. 10 (A),
462 B70s0.14 highly reduced residual carbon particles at a higher mixing intensity, and was
463 superior to PACl-70 for all mixing conditions tested. The superiority of B70s0.14 to PACl-
464 70 was also confirmed in the experiments where natural water supplemented with SPAC was
465 used (Fig. 10 (B)). Moreover, the trend that high G_FT_F results in low concentration of residual
466 carbon particles, which described in the section 3.3, was also observed in the data of natural
467 water. In case of very high G_FT_F (60,000) applied, very low concentrations of residual carbon
468 particles were attained with both B70s0.14 and PACl-70 and their difference was small.
469 Residual carbon particle concentrations obtained in the experiments using river water (Fig.
470 10 (B)) were somewhat lower than those using filtered tap water (Fig. 10 (A)). However the
471 effect of organic matter concentrations and turbidity should not be inferred by the comparison
472 of these two data because the two waters differed in ionic composition as well as organic
473 matter concentrations and turbidity, all of which affect coagulation performance.
474
475 The PACls produced by $Al(OH)_3$-dissolution, including B70s0.14, which showed the high
476 performance on the reduction of residual SPAC after CSF, contained Alc as the main
477 component. However, the percentages of Ala, Alb, and Alc were almost the same as those of
478 the Alc-type PACls prepared by base-titration (Fig. 17S, SI), which were not effective
479 coagulants. This means that the Al species distribution determined by the ferron method is
480 not informative in evaluating the ability for coagulation treatment targeting SPAC, in
481 particular the ability of floc formation. Base-titration required a high temperature when
482 adjusting the basicity and resulted in a high salt (Na and Cl) content in comparison to
483 $Al(OH)_3$-dissolution. These differences were inferred to influence the ability of floc
484 formation. Studies on PACl produced by $Al(OH)_3$-dissolution are scarcely seen, and further

485 investigations are expected.

486

487

488 **4. Conclusions**

489

490 The addition of SPAC in water treatment is a promising technology to remove organic
491 contaminants, but efficient removal of the loaded SPAC is needed. In this study, key control
492 points to attain the high log removal rates of SPAC and to reduce residual SPAC particles at
493 trace concertation levels of 100 to 1000 particles/mL in treated water were examined, and
494 their background mechanisms were discussed, focusing on the process points of coagulation-
495 flocculation and coagulants in CSF. The following conclusions were obtained.

496

497 1) A sufficiently large G value in flash mixing for the first step of coagulation was clearly a
498 dominant factor for minimizing residual carbon particle concentration in the treated water
499 after the fourth step of sand filtration. Adequate mixing for coagulation would enable
500 complete dispersion of coagulant thereby reducing the number of particles that were not
501 charge-neutralized. Such particles would pass through the sand filter into the treated water.

502

503 2) Commercially available PACls were compared with each other: high-basicity PACl
504 (basicity 70%) was more effective in removing residual carbon particles. It was because the
505 high-basicity PACl had a high charge neutralizing capacity to destabilize many particles,
506 though it formed flocs slowly. However, this superiority of high-basicity PACl was provided
507 by the sufficient flash mixing. Without sufficient flash mixing, not only the removal rate
508 decreased but also the high-basicity PACl became inferior to conventional-basicity PACl.

509

3) High-basicity PACl with SO_4/Al=0.14 reduced residual carbon particles down to the minimum concentration. Such a high performance PACl coagulant was produced by using $Al(OH)_3$-dissolution, and the dominant Al species was Alc determined by the ferron method. In contrast, Alb and Alc type PACls produced by base-titration had a high positive charge capacity and were poor at forming floc particles due to lack of bridge-forming ability; this was true even if they were used at a large dosage or the optimal dosage in terms of charge neutralization.

Acknowledgments

This study was supported by a Grant-in-Aid for Scientific Research S (16H06362) from the Japan Society for the Promotion of Science.

References

Aguilar, M.I., Sáez, J., Lloréns, M., Soler, A. and Ortuño, J.F. (2003) Microscopic observation of particle reduction in slaughterhouse wastewater by coagulation–flocculation using ferric sulphate as coagulant and different coagulant aids. Water Research 37(9), 2233-2241.

Amaral, P., Partlan, E., Li, M., Lapolli, F., Mefford, O.T., Karanfil, T. and Ladner, D.A. (2016) Superfine powdered activated carbon (S-PAC) coatings on microfiltration membranes: Effects of milling time on contaminant removal and flux. Water Research 100, 429-438.

American Society of Civil Engineers and American Water Works Association (1998) Water Treatment Plant Design, McGraw-Hill.

American Water Works Association and American Society of Civil Engineers (2012) Water Treatment Plant Design 5/E, Mcgraw-hill.

Amirtharaja, A. and O'Melia, C.R. (1990) Water Quality & Treatment 4th ed. Pontius, F.W. (ed), McGraw-Hill.

Ando, N., Matsui, Y., Kurotobi, R., Nakano, Y., Matsushita, T. and Ohno, K. (2010) Comparison of natural organic matter adsorption capacities of super-powdered activated carbon and powdered activated Carbon. Water Research 44(14), 4127-4136.

Bonvin, F., Jost, L., Randin, L., Bonvin, E. and Kohn, T. (2016) Super-fine powdered activated carbon (SPAC) for efficient removal of micropollutants from wastewater treatment plant effluent. Water Research 90, 90-99.

Bureau of Waterworks Tokyo Metropolitan Government (2014) Personal communication.

Ellerie, J.R., Apul, O.G., Karanfil, T. and Ladner, D.A. (2013) Comparing graphene, carbon nanotubes, and superfine powdered activated carbon as adsorptive coating materials for microfiltration membranes. Journal of Hazardous Materials 261(0), 91-98.
Gao, B.-Y., Chu, Y.-B., Yue, Q.-Y., Wang, B.-J. and Wang, S.-G. (2005) Characterization and coagulation of a polyaluminum chloride (PAC) coagulant with high Al13 content. J Environ Manage 76(2), 143-147.
Gao, B. and Yue, Q. (2005) Effect of SO42-/Al3+ ratio and OH−/Al3+ value on the characterization of coagulant poly-aluminum-chloride-sulfate (PACS) and its coagulation performance in water treatment. Chemosphere 61(4), 579-584.
Hendricks, D. (2010) Fundamentals of Water Treatment Unit Processes: Physical, Chemical, and Biological, Taylor & Francis.
Itoh, Y. and Sato, K. (1995) Production of Sulfate-containing Basic Al Chloride, Japan Patent Office, 1995-033432
Jia, He, F. and Liu (2004) Synthesis of Polyaluminum Chloride with a Membrane Reactor: Operating Parameter Effects and Reaction Pathways. Industrial & Engineering Chemistry Research 43(1), 12-17.
Kan, C., Huang, C. and Pan, J.R. (2002) Time requirement for rapid-mixing in coagulation. Colloids and Surfaces A: Physicochemical and Engineering Aspects 203(1), 1-9.
Kimura, M., Matsui, Y., Kondo, K., Ishikawa, T.B., Matsushita, T. and Shirasaki, N. (2013) Minimizing residual aluminum concentration in treated water by tailoring properties of polyaluminum coagulants. Water Research 47(6), 2075-2084.
Letterman, R.D. and Yiacoumi, S. (2011) Water quality and treatment: a handbook of community water supplies. Edzwald, J.K. and American Water Works Association (eds), McGraw-Hill.
Lin, J.-L., Chin, C.-J.M., Huang, C., Pan, J.R. and Wang, D. (2008) Coagulation behavior of Al13 aggregates. Water Research 42(16), 4281-4290.
Lin, J.-L., Pan, J.R. and Huang, C. (2013) Enhanced particle destabilization and aggregation by flash-mixing coagulation for drinking water treatment. Separation and Purification Technology 115, 145-151.
Matsui, Y., Fukuda, Y., Murase, R., Aoki, N., Mima, S., Inoue, T. and Matsushita, T. (2004) Micro-ground powdered activated carbon for effective removal of natural organic matter during water treatment. Water Science & Technology: Water Supply 4(4), 155-163.
Matsui, Y., Hasegawa, H., Ohno, K., Matsushita, T., Mima, S., Kawase, Y. and Aizawa, T. (2009) Effects of super-powdered activated carbon pretreatment on coagulation and trans-membrane pressure buildup during microfiltration. Water Research 43(20), 5160-5170.
Matsui, Y., Shirasaki, N., Yamaguchi, T., Kondo, K., Machida, K., Fukuura, T. and Matsushita, T. (2017) Characteristics and components of poly-aluminum chloride coagulants that enhance arsenate removal by coagulation: Detailed analysis of aluminum species. Water Research 118, 177-186.
Matsui, Y., Yoshida, T., Nakao, S., Knappe, D.R.U. and Matsushita, T. (2012) Characteristics of competitive adsorption between 2-methylisoborneol and natural organic matter on superfine and conventionally sized powdered activated carbons. Water Research 46(15), 4741-4749.
Nakazawa, Y., Matsui, Y., Hanamura, Y., Shinno, K., Shirasaki, N. and Matsushita, T. (2018) Identifying, counting, and characterizing superfine activated-carbon particles remaining after coagulation, sedimentation, and sand filtration. Water Research 138, 160-168.

592 Pan, L., Nishimura, Y., Takaesu, H., Matsui, Y., Matsushita, T. and Shirasaki, N. (2017)
593 Effects of decreasing activated carbon particle diameter from 30 μm to 140 nm on
594 equilibrium adsorption capacity. Water Research 124, 425-434.
595 Parker, D.R. and Bertsch, P.M. (1992) Identification and quantification of the "Al13"
596 tridecameric aluminum polycation using ferron. Environmental Science & Technology
597 26(5), 908-914.
598 Parthasarathy, N. and Buffle, J. (1985) Study of polymeric aluminium(III) hydroxide
599 solutions for application in waste water treatment. Properties of the polymer and optimal
600 conditions of preparation. Water Research 19(1), 25-36.
601 Partlan, E., Davis, K., Ren, Y., Apul, O.G., Mefford, O.T., Karanfil, T. and Ladner, D.A.
602 (2016) Effect of bead milling on chemical and physical characteristics of activated carbons
603 pulverized to superfine sizes. Water Research 89, 161-170.
604 Sato, F. and Matsuda, S. (2009) Novel basic aluminum chloride, its manufacturing method
605 and its application, Japan Patent Office, 2009-203125.
606 Shi, B., Li, G., Wang, D. and Tang, H. (2007) Separation of Al13 from polyaluminum
607 chloride by sulfate precipitation and nitrate metathesis. Separation and Purification
608 Technology 54(1), 88-95.
609 Wang, D., Sun, W., Xu, Y., Tang, H. and Gregory, J. (2004) Speciation stability of
610 inorganic polymer flocculant–PACl. Colloids and Surfaces A: Physicochemical and
611 Engineering Aspects 243(1-3), 1-10.
612 Wang, D., Tang, H. and Gregory, J. (2002) Relative Importance of Charge Neutralization
613 and Precipitation on Coagulation of Kaolin with PACl: Effect of Sulfate Ion.
614 Environmental Science & Technology 36(8), 1815-1820.
615 Wu, X., Ge, X., Wang, D. and Tang, H. (2007) Distinct coagulation mechanism and model
616 between alum and high Al13-PACl. Colloids and Surfaces A: Physicochemical and
617 Engineering Aspects 305(1-3), 89-96.
618 Yan, M., Wang, D., Ni, J., Qu, J., Chow, C.W.K. and Liu, H. (2008) Mechanism of natural
619 organic matter removal by polyaluminum chloride: Effect of coagulant particle size and
620 hydrolysis kinetics. Water Research 42(13), 3361-3370.
621 Younker, J.M. and Walsh, M.E. (2016) Effect of adsorbent addition on floc formation and
622 clarification. Water Research 98, 1-8.
623 Zhao, B., Wang, D., Li, T., Chow, C.W.K. and Huang, C. (2010) Influence of floc structure
624 on coagulation–microfiltration performance: Effect of Al speciation characteristics of
625 PACls. Separation and Purification Technology 72(1), 22-27.
626 Zhao, H., Peng, J., Lin, S. and Zhang, Y. (2009) Covalently Bound Organic Silicate
627 Aluminum Hybrid Coagulants: Preparation, Characterization, and Coagulation Behavior.
628 Environmental Science & Technology 43(6), 2041-2046.
629
630
631

Table 1. Activated carbon particle size. The median diameters were determined by laser light diffraction and scattering.

Activated carbon		Median diameter (μm)
PAC		13.7
SPAC	$SPAC_1$	0.96
	$SPAC_2$	0.90

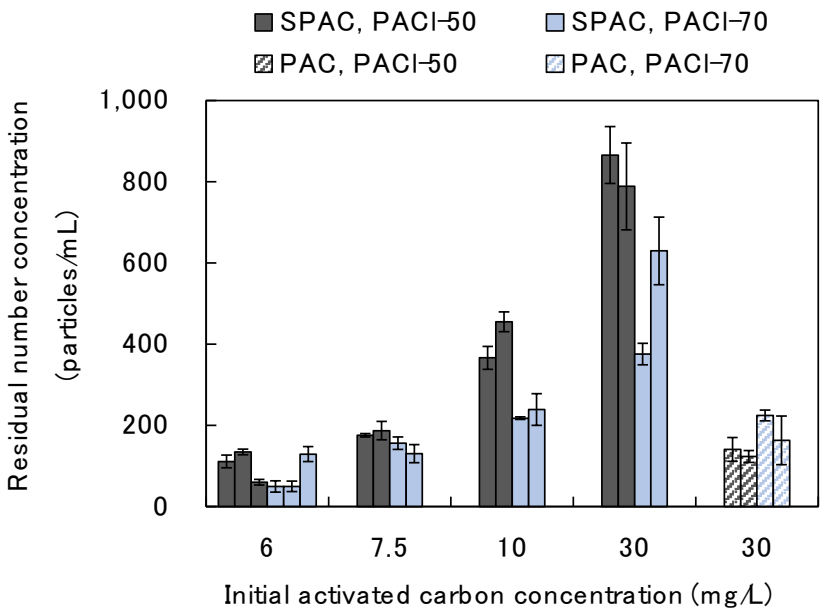

Figure 1. Particle number concentration of residual activated carbon vs. initial activated carbon concentration at a fixed mixing intensity ($G_T T_T$: 39,000, G_F: 600 s^{-1}, T_F: 20 s; G_{S1}: 50 s^{-1}, T_{S1}: 300 s, G_{S2}: 20 s^{-1}, T_{S2}: 300 s, G_{S3}: 10 s^{-1}, T_{S3}: 600 s). PAC and $SPAC_1$ were used. Error bars indicate standard deviations of measurements.

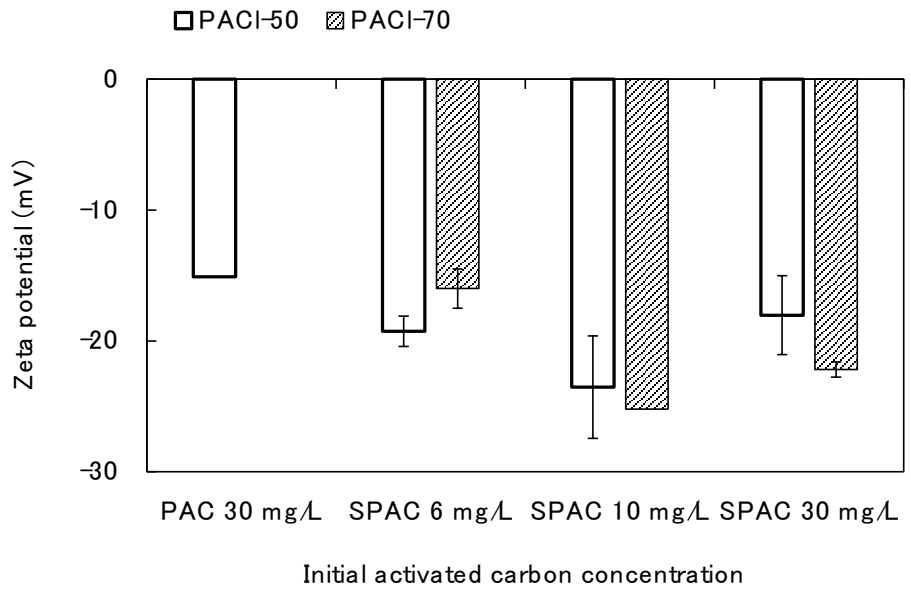

Figure 2. Zeta potentials of residual carbon particles in sand-filtrate vs. initial activated carbon concentration. Experimental conditions were the same as those described for Fig. 1. The number of measurements was described as follows: with PACl-70, two measurements for SPAC 6 mg/L and 30 mg/L, and one measurement for SPAC 10 mg/L; with PACl-50, three measurements for SPAC 30 mg/L, two measurements for SPAC 6 mg/L and 10 mg/L, and one measurement for PAC 30 mg/L. Error bars indicate standard deviations of measurements.

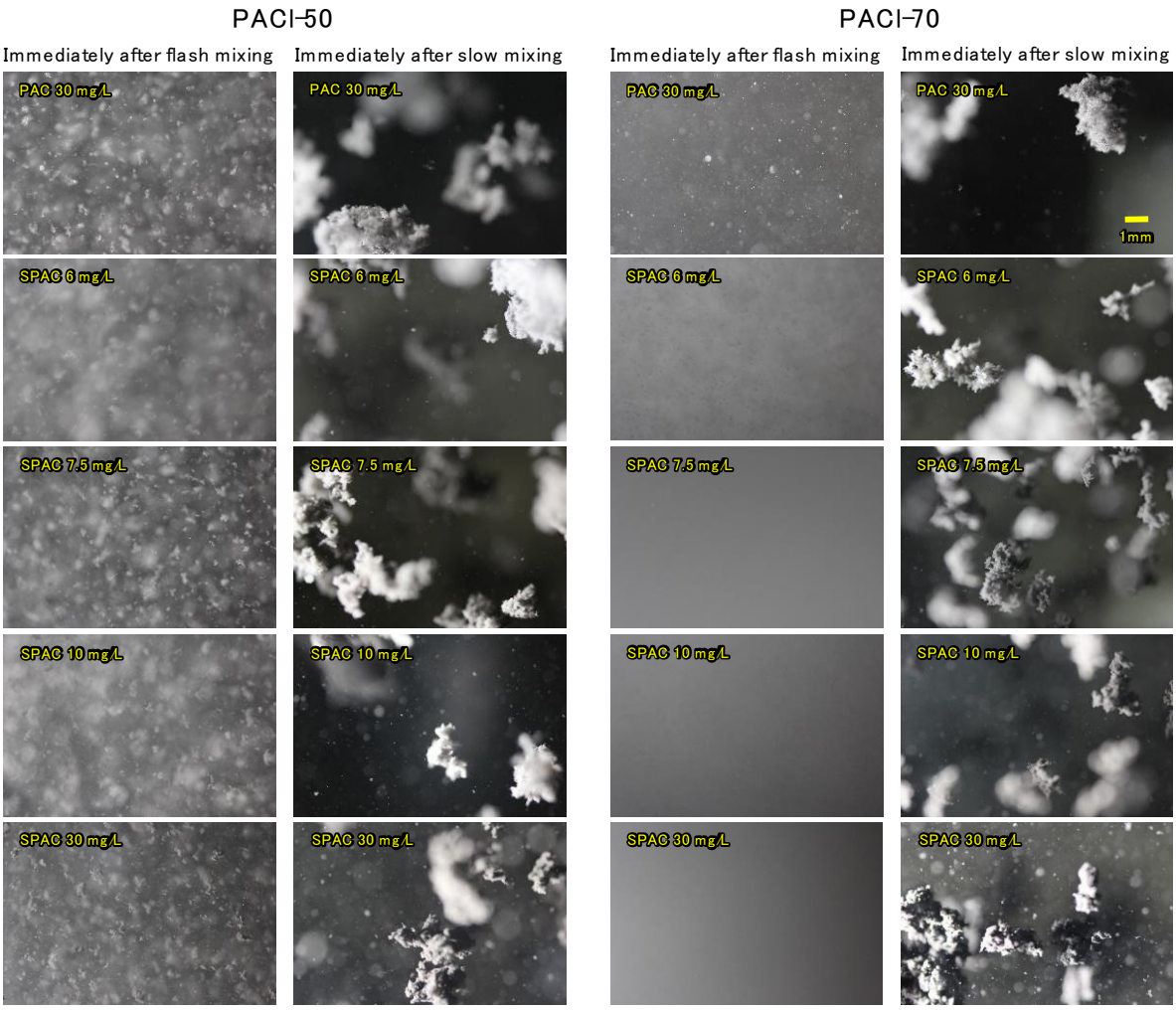

Figure 3. Photos of floc particles during the experiments of Fig. 1. The two columns of the left side are experiments using PACl-50. The two columns of the right side are experiments using PACl-70. The photos in the first column in each set of two rows were taken immediately after flash mixing was finished. The photos in the second column in each set of two rows were taken immediately after slow mixing was finished.

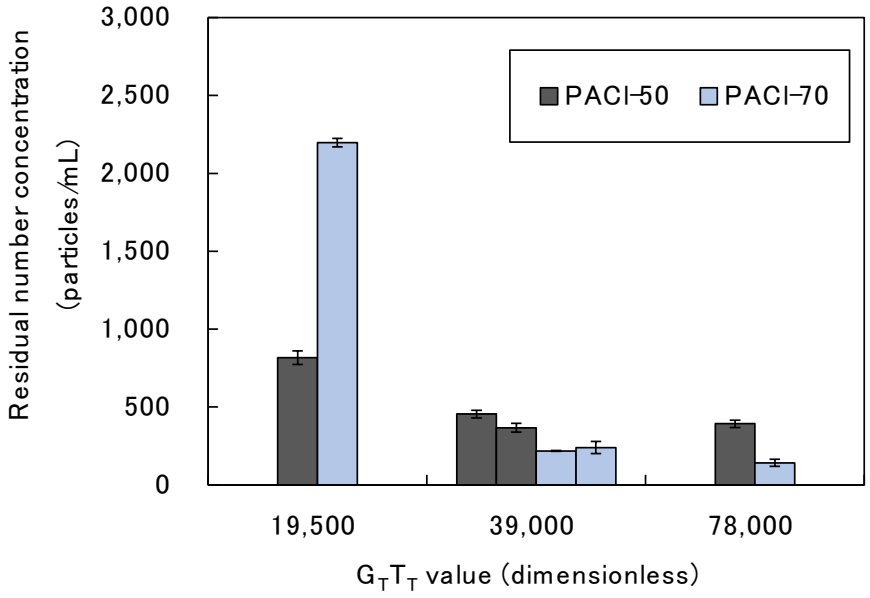

Figure 4. Effect of total mixing intensity (G_TT_T value=G_FT_F value of flash mixing+G_ST_S value of slow mixing) on the particle number concentration of residual carbon. $SPAC_1$ was used. Initial $SPAC_1$ concentration was 10 mg/L. Details of the mixing conditions are shown in Table 2S of SI. The number of experiments for each mixing condition was described as follows: with total GT 39,000, two experiments; with total GT 19,500 and 78,000, one experiment each. Error bars indicate standard deviations of measurements.

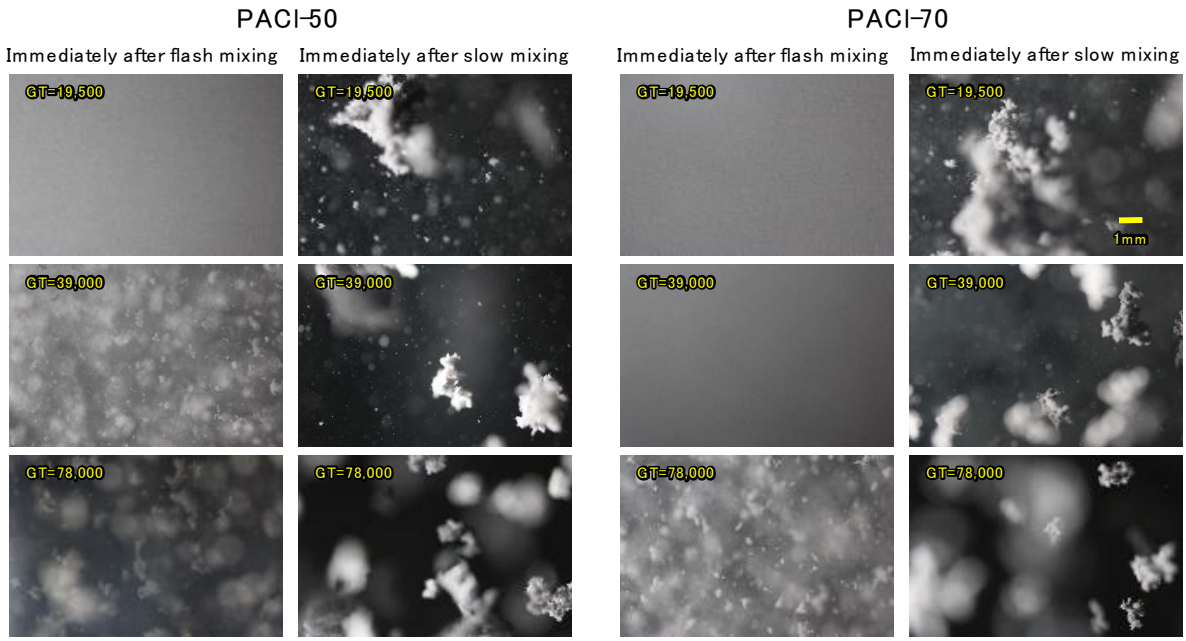

Figure 5. Photos of floc particles during the experiments of Fig. 4. The two columns of the left side are experiments using PACl-50. The two columns of the right side are experiments using PACl-70. The photos in the first column in each set of two rows were taken immediately after flash mixing was finished. The photos in the second columns in each set of two rows were taken immediately after slow mixing was finished.

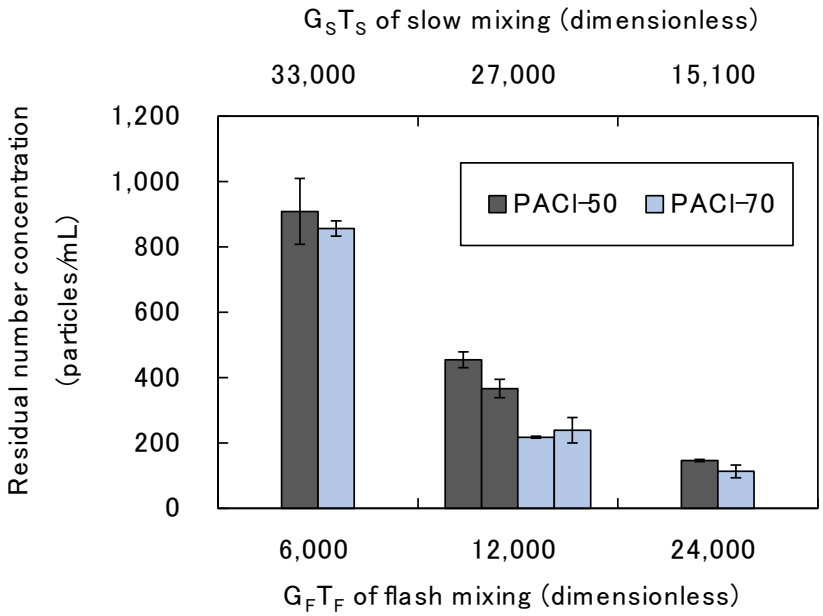

Figure 6. Effect of mixing intensity in flash and slow mixing on the particle number concentration of residual carbon at a fixed total mixing intensity. $SPAC_1$ was used. Initial $SPAC_1$ concentration was 10 mg/L. G_TT_T value (=G_FT_F of flash mixing+G_ST_S of slow mixing) was fixed at about 39,000. Details of the mixing conditions are shown in Table 2S of SI. The number of experiments for each mixing condition was described as follows: with G_TT_T 39,000 (G_FT_F=12,000), two experiments; with G_TT_T 39,000 (G_FT_F=6,000) and 39,100 (G_FT_F=24,000), one experiment. Error bars indicate standard deviations of measurements.

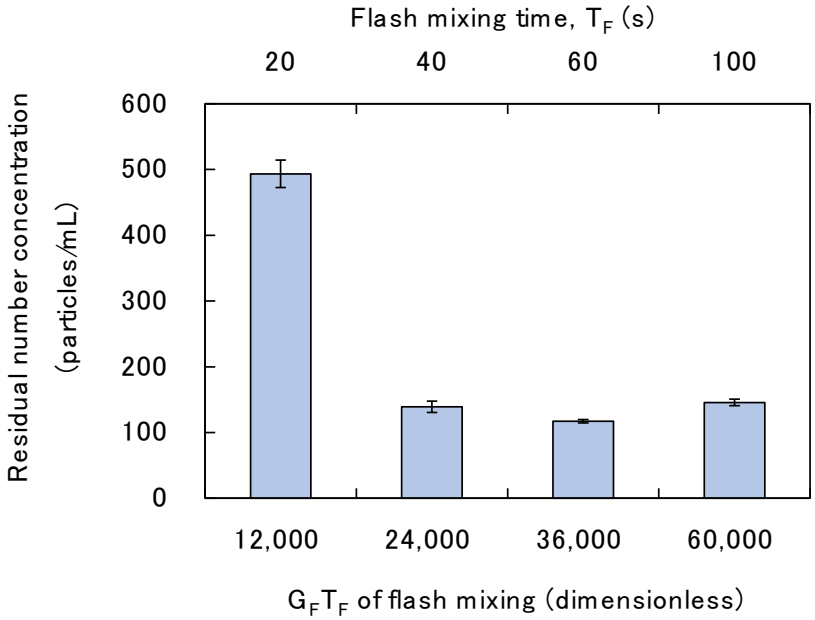

Figure 7. Effect of flash mixing time (T_F) on the particle number concentration of residual carbon. $SPAC_2$ was used. Initial $SPAC_2$ concentration was 10 mg/L. PACl-70 was used. G_F value was fixed at 600 s^{-1}. G_ST_S of slow mixing=15,100. Details of the mixing conditions are shown in Table 2S of SI. Error bars indicate standard deviations of measurements.

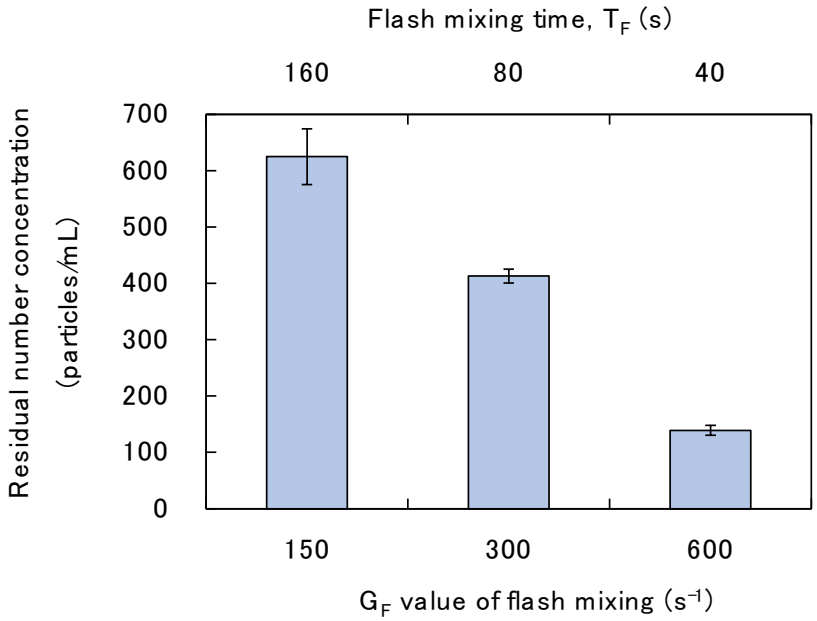

Figure 8. Effect of mixing speed (G_F) and time (T_F) in flash mixing on the particle number concentration of residual carbon at a fixed flash mixing intensity (G_FT_F=24,000) and a fixed slow mixing intensity (G_ST_S=15,100). $SPAC_2$ was used. Initial $SPAC_2$ concentration was 10 mg/L. PACl-70 was used. Error bars indicate standard deviations of measurements.

Table 2. Coagulants made by $Al(OH)_3$-dissolution.

Name	Basicity	SO_4/Al	Cl/Al	Na/Al	Al content	Titrating process	
						Time	Temperature
	%	mole ratio	mole ratio	mole ratio	mol/L	h	℃
B70ns	70	0.00	1.68	0.78	2.0	1.0	50
B70s0.11	70	0.11	1.46	0.79	2.0	1.0	50
B70s0.12	70	0.12	1.36	0.69	2.2	1.0	50
B70s0.13	70	0.13	1.36	0.72	2.0	1.3	50
B70s0.14-1	70	0.14	1.43	0.79	2.1	1.3	50
B70s0.14-2	70	0.14	1.44	0.81	2.1	1.4	50
B70s0.14-3	70	0.14	1.37	0.75	1.9	1.4	50
B70s0.14-4	70	0.14	1.37	0.75	1.9	1.4	50
B70s0.15-1	70	0.15	1.31	0.71	2.2	1.4	50~77
B70s0.15-2	70	0.15	1.29	0.68	2.1	1.3	50~77
B70s0.17	70	0.17	1.34	0.78	2.1	1.0	50~80

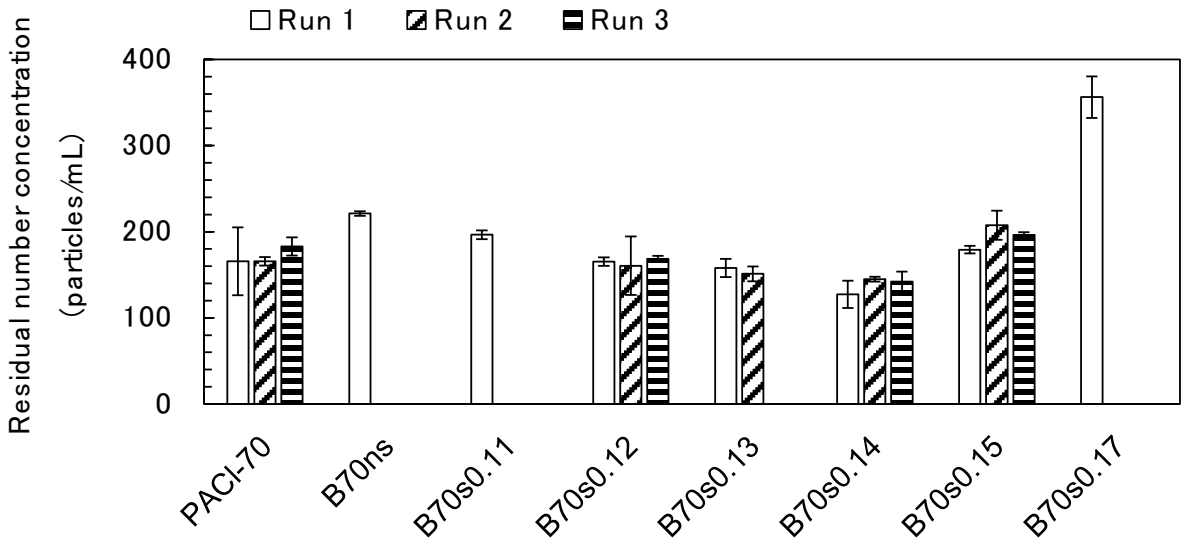

Figure 9. Particle number concentration of residual carbon after CSFs with various PACls. $SPAC_1$ was used. Initial $SPAC_1$ concentration was 10 mg/L. G_TT_T value was fixed at 39,000. Three runs were conducted for PACl-70, B70s0.12, B70s0.14 (B70s0.14-1 was used for all Runs), and B70s0.15 (B70s0.15-1 was used for Run 1, and B70s0.15-2 was used for Run 2 and 3). Two runs were for B70s0.13. One run was conducted for B70ns, B70s0.11, and B70s0.17. Error bars indicate standard deviations of three measurements.

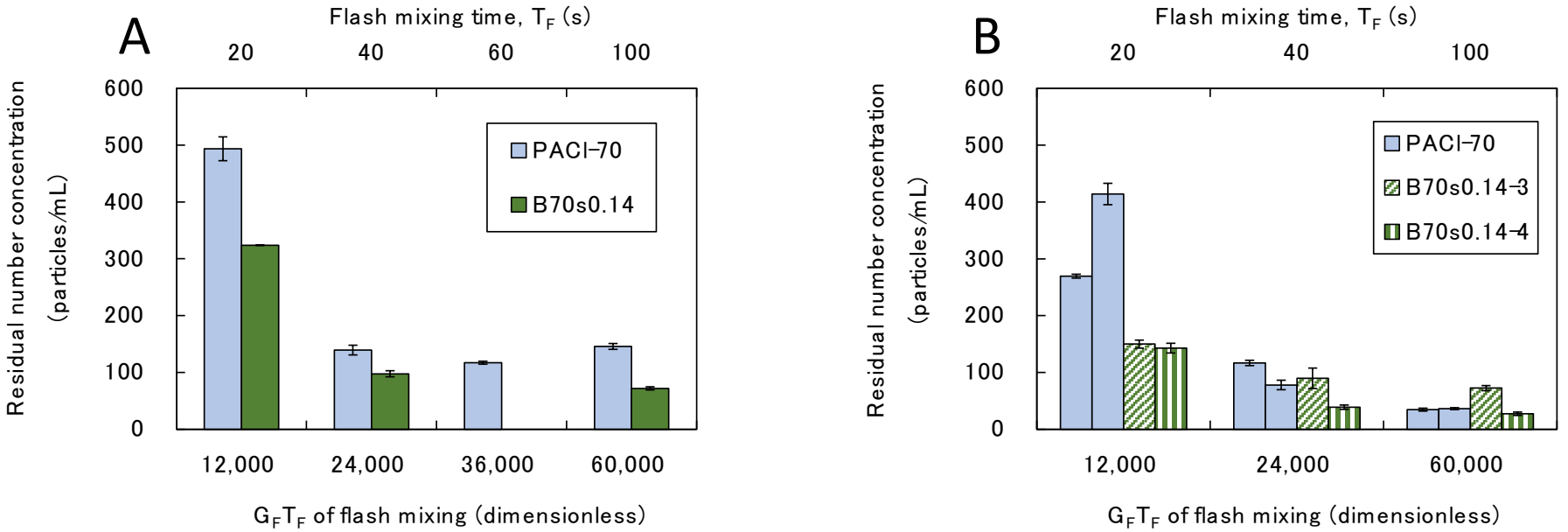

Figure 10. Effect of flash mixing time on the particle number concentration of residual carbon. $SPAC_2$ was used. Initial $SPAC_2$ concentration was 10 mg/L. G_F value was fixed at 600 s^{-1}. G_ST_S of slow mixing was 15,100. Details of the mixing conditions are shown in Table 2S of SI. Error bars indicate standard deviations of measurements. (A) Filtered tap water supplemented with $SPAC_2$ was used as raw water; PACl-70 and B70s0.14-2 were used as coagulant. (B) River water (turbidity 2.5 NTU and TOC 0.6 mg/L) supplemented with $SPAC_2$ was used as raw water; PACl-70, B70s0.14-3, and B70s0.14-4 were used.

Supplementary Information

Minimizing residual black particles in sand filtrate when applying super-fine powdered activated carbon: coagulants and coagulation conditions

Yoshifumi Nakazawa [a], Yoshihiko Matsui [b*], Yusuke Hanamura [a], Koki Shinno [a], Nobutaka Shirasaki [b], and Taku Matsushita [b]

a Graduate School of Engineering, Hokkaido University, N13W8, Sapporo 060-8628, Japan
b Faculty of Engineering, Hokkaido University, N13W8, Sapporo 060-8628, Japan

* Corresponding author. Tel./fax: +81-11-706-7280
E-mail address: matsui@eng.hokudai.ac.jp

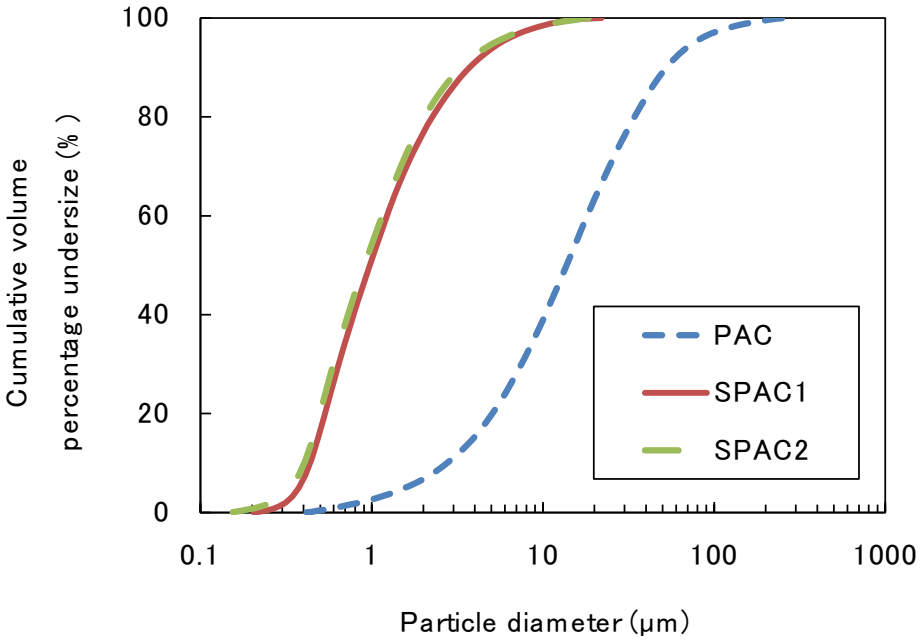

Figure 1S. Particle size distributions of PAC, $SPAC_1$, and $SPAC_2$.

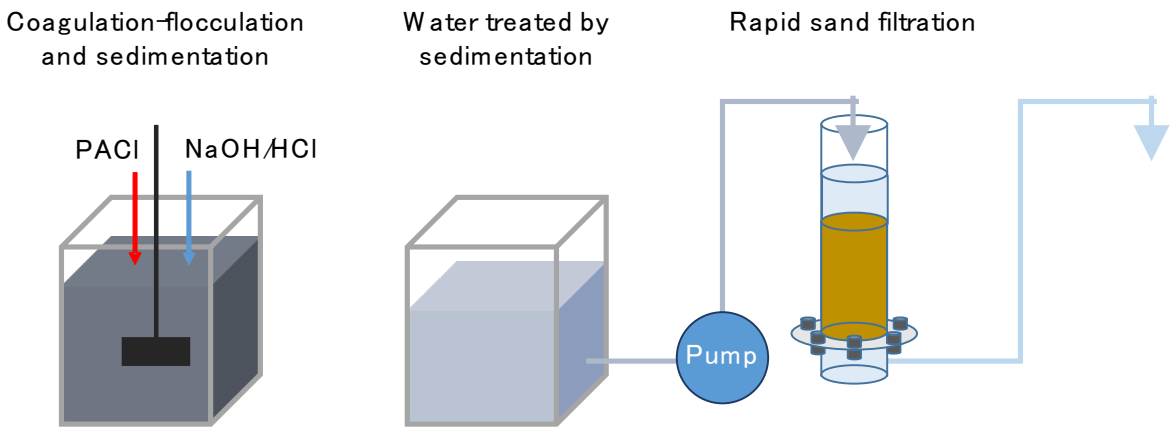

Figure 2S. Schematic diagram of the experimental setup for the coagulation-flocculation, sedimentation, and sand filtration experiment.

Calculation of G (velocity gradient) value

The mean velocity gradient G (s^{-1}) is defined as a function of P, μ, and V as follows.

$$G = \sqrt{\frac{P}{\mu V}} \qquad (1)$$

where P is power consumed by the agitating impeller in a mixing vessel (W), μ is the viscosity of water (Pa s), and V (m^3) is the volume of the water in the mixing vessel.

Power consumption is given by the product of force acting on an impeller blade and its moving velocity. Velocity and force acting on the blade of the impeller varies radially such that the tip of the blade moves fastest (tip speed) and the force acting on the tip is strongest, but the root end of the blade moves slowest and its force is smallest. Therefore, power consumed by a rotating impeller blade is given by:

$$P_B = \int v\, p dA \qquad (2)$$

$$p = \frac{1}{2}\rho_w C_d v^2 \qquad (3)$$

where, P_B is the power required to move a blade (W), v is the velocity of the moving blade (m/s), p is the pressure acting vertically on the blade (Pa), A is the area of blade (m^2), ρ_w is the density of fluid (kg/m^3), and C_d is drag coefficient (dimensionless).

For a flat rectangular blade shown in Fig. 3S,

$$v = 2\pi(1 - K_r)xN_s \qquad (4)$$

$$dA = hdx \qquad (5)$$

where, K_r is (dimensionless), x is the radial distance from the impeller center (m), N_s is rotational speed (rps), and h is the height of a impeller blade (m).

By substituting equations (3), (4) and (5) into (2):

$$P_B = \int_{r_1}^{r_2} \frac{1}{2}\rho_w C_d [2\pi(1 - K_r)xN_s]^3 h dx = \rho_w C_d [\pi(1 - K_r)N_s]^3 h({r_2}^4 - {r_1}^4) \qquad (6)$$

The total power input to the mixing tank having multiple impeller blades is given by:

$$P = nP_B = n\rho_w C_d [\pi N_s]^3 h({r_2}^4 - {r_1}^4) \qquad (7)$$

where, n is the number of impeller blades in a mixer.

Substituting Eq. (10) into Eq. (1) gives,

$$G = \sqrt{\frac{n\rho_w C_d \pi^3 (1 - K_r)^3 {N_s}^3 h({r_2}^4 - {r_1}^4)}{\mu V}}. \qquad (8)$$

The values used for the calculation of *G* values by equation (8) were summarized in Table 1S.

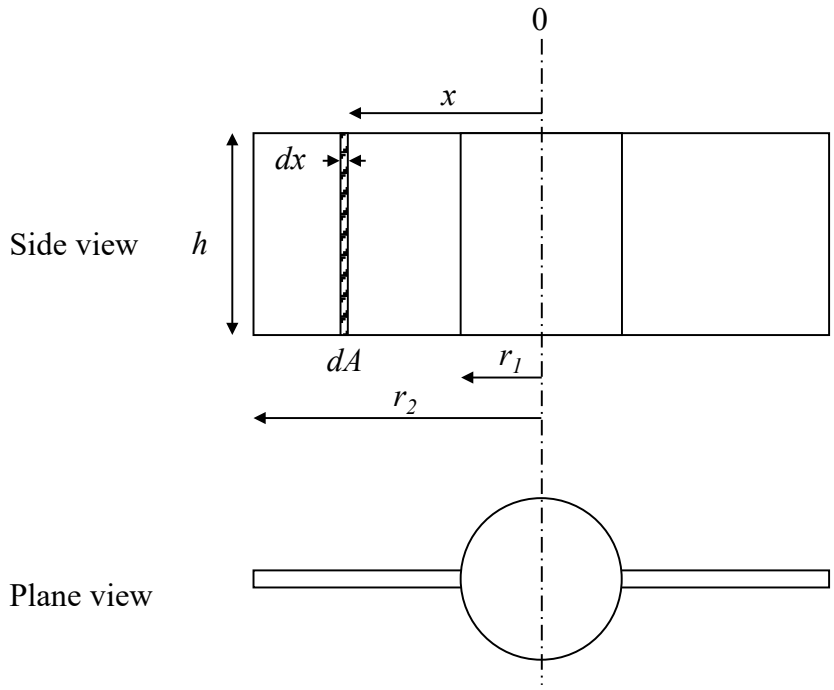

Figure 3S. Schematic diagram of mixing blade for the calculation of G value.

Table1S. Parameter values used for G value calculation.

Parameter symbol	Unit	Value
V	m^3	0.004
μ	Pa s	1.005×10^{-3}
h	m	0.035
r_1	m	0.014
r_2	m	0.05
ρ_w	kg m^{-3}	9.982×10^2
C_d	dimensionless	1.5
K_r	dimensionless	0
n	dimensionless	4
N_S	rps	from 0.22 to 3.28

Table 2S. The experimental conditions of coagulation in CSF experiments.

	Activated carbon		Coagulant		Flash mixing		Slow mixing						Flash + slow mixing
	Name	Initial concentration (mg L^{-1})	Name	Dosage (mg-Al L^{-1})	G_F (s^{-1})	T_F (s)	G_{S1} (s^{-1})	T_{S1} (s)	G_{S2} (s^{-1})	T_{S2} (s)	G_{S3} (s^{-1})	T_{S3} (s)	$G_T T_T$ (dimensionless)
Fig. 1 Fig. 6S Fig. 7S	PAC and $SPAC_1$	30 (PAC) and 6~30 ($SPAC_1$)	PACl-50 and PACl-70	4	600	20	50	300	20	300	10	600	39,000
Fig. 4 Fig. 9S	$SPAC_1$	10	PACl-50 and PACl-70	4	600	10	50	150	20	150	10	300	19,500
					600	20	50	300	20	300	10	600	39,000
					600	40	50	600	20	600	10	1,200	78,000
Fig. 6	$SPAC_1$	10	PACl-50 and PACl-70	4	600	10	50	375	20	375	10	675	39,000
					600	20	50	300	20	300	10	600	39,000
					600	40	50	170	20	170	10	320	39,100
Fig. 7	$SPAC_2$	10	PACl-70	4	600	20	50	170	20	170	10	320	27,100
					600	40	50	170	20	170	10	320	39,100
					600	60	50	170	20	170	10	320	51,100
					600	100	50	170	20	170	10	320	75,100
Fig. 8	$SPAC_2$	10	PACl-70	4	150	160	50	170	20	170	10	320	39,100
					300	80	50	170	20	170	10	320	39,100
					600	40	50	170	20	170	10	320	39,100
Fig. 9	$SPAC_1$	10	PACl-70 and PACls by $Al(OH)_3$-solution	4	600	20	50	300	20	300	10	600	39,000
Fig. 10	$SPAC_2$	10	PACl-70 and B70s0.14	4	600	20	50	170	20	170	10	320	27,100
					600	40	50	170	20	170	10	320	39,100
					600	60	50	170	20	170	10	320	51,100
					600	100	50	170	20	170	10	320	75,100
Fig. 10S Fig. 11S	$SPAC_1$	10	PACl-50 and PACl-70	1.5~8	600	40	50	600	20	600	10	1,200	78,000

G and T stand for velocity gradient and mixing time, respectively. Subscripts F, S, and the numbers after S mean flash mixing, slow mixing, and the order of the slow mixing part, respectively.

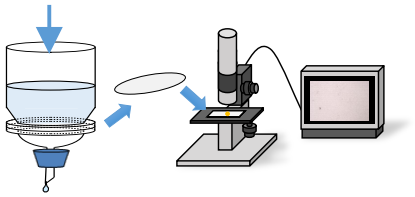

Figure 4S. Schematic diagram of the experimental setup for membrane filtration and microscopic image analysis.

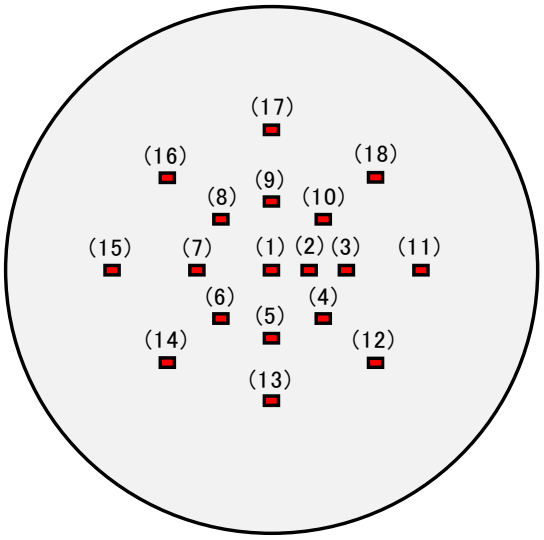

Figure 5S. The position of observation zones on a membrane filter. The observation was conducted with 18 zones in the case that the particle number concentration was expected to be lower than 200 particles/mL. In the other case, the observation was conducted with 9 zones (zone numbers 1 and from 3 to 10).

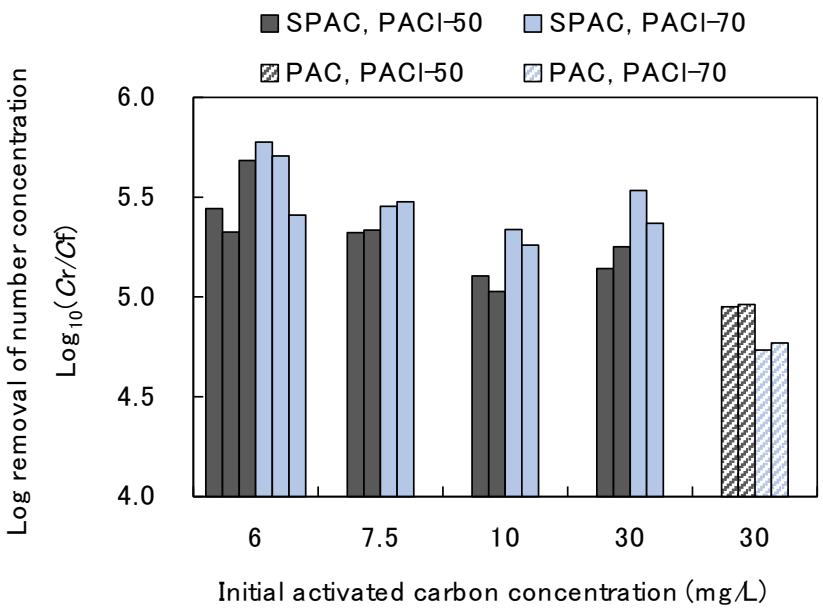

Figure 6S. Removal rate in terms of particle number concentration after CSF in the experiments of Fig. 1. *C*r and *C*f indicate the particle number concentration of carbon in raw water and sand filtrate, respectively.

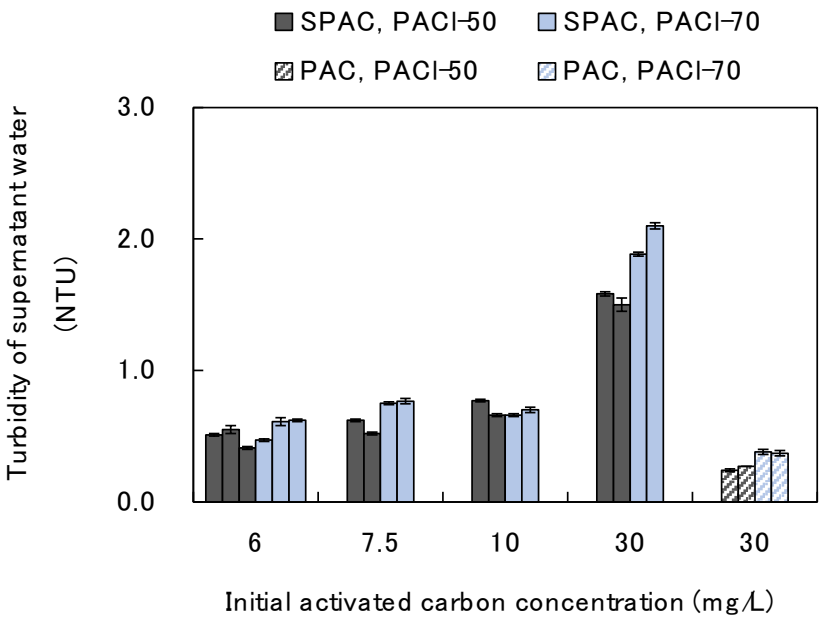

Figure 7S. Turbidity of supernatant after coagulation, flocculation, and sedimentation in the experiments of Fig. 1. Error bars indicate standard deviations of measurements.

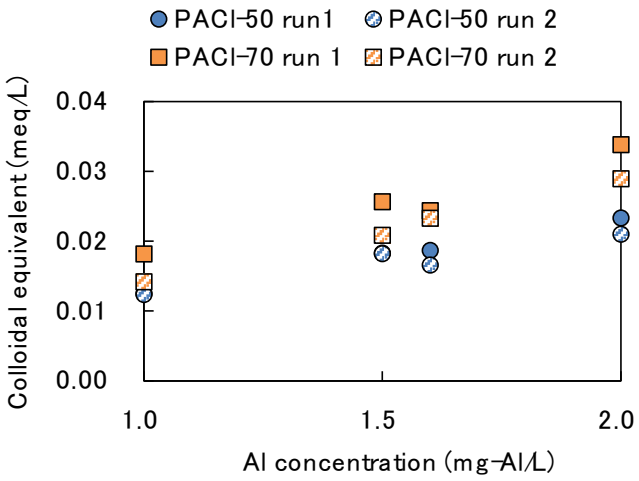

Figure 8S. Colloid charge capacity of PACl-50 and PACl-70 (Matsui et al. 2017).

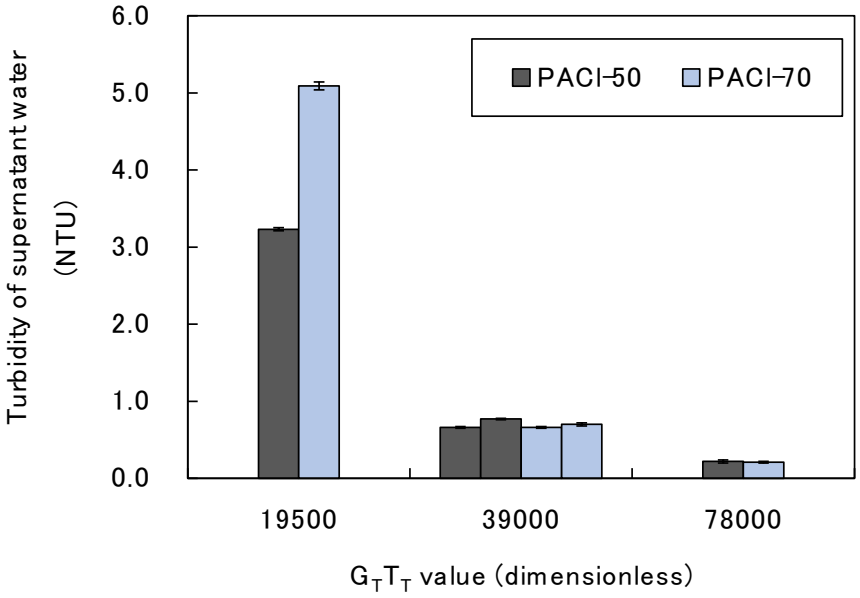

Figure 9S. Turbidity of supernatant after coagulation, flocculation, and sedimentation in the experiments of Fig. 4. Error bars indicate standard deviations of measurements.

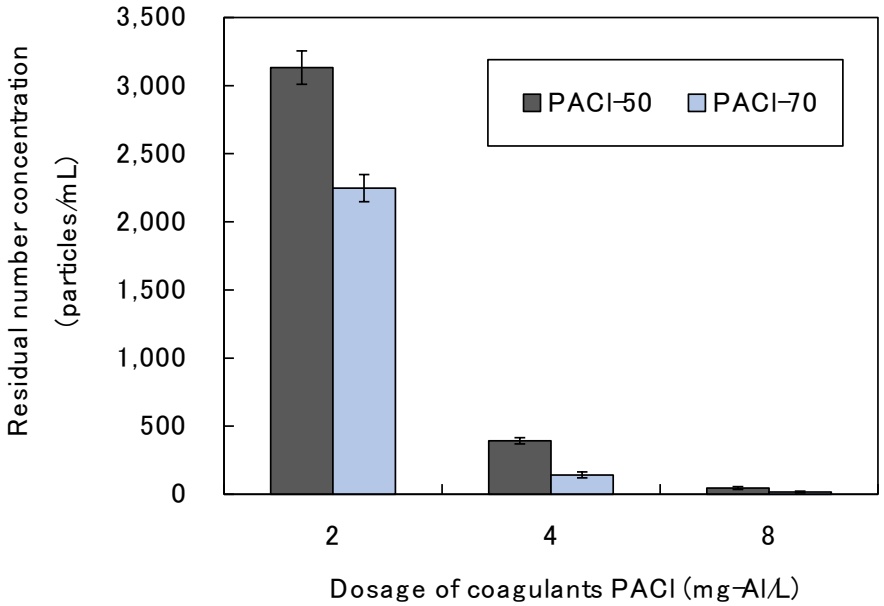

Figure 10S. Effect of coagulant dosage on the particle number concentration of residual carbon in sand filtrate. $SPAC_1$ was used. Initial $SPAC_1$ concentration was 10 mg/L. G_TT_T value was fixed at 78,000 (G_FT_F=24,000, G_ST_S=54,000). Error bars indicate standard deviations of measurements.

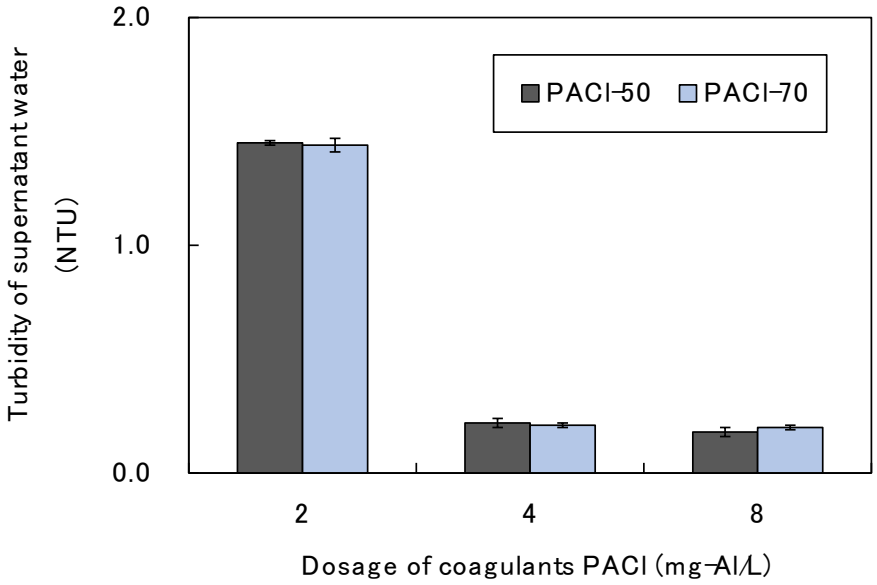

Figure 11S. Turbidity of supernatant after coagulation, flocculation, and sedimentation in the experiments of Fig. 10S. Error bars indicate standard deviations of measurements.

Table 3S. Coagulants made by base-titration.

Name	Basicity	SO_4/Al	Cl/Al	Na/Al	Al content	Heating process	
						Time	Temperature
	%	molar ratio	molar ratio	molar ratio	mol/L	h	℃
B65ns	65	0	3.00	1.95	0.1		
B65ns-heat	65	0	3.00	1.95	0.1	5.0	121
B79s0.10-1	79	0.10	2.80	2.38	0.04		
B79s0.10-2-heat	79	0.10	2.80	2.38	0.09	(5.0)	(121)
B80ns-1	80	0	3.00	2.40	0.05		
B80ns-2	80	0	3.00	2.40	0.1		
B80ns-2-heat	80	0	3.00	2.40	0.1	0.33	120
B82s0.11	82	0.11	2.79	2.45	0.1		
B82s0.11-heat	82	0.11	2.79	2.45	0.1	72	90~95
B88s0.10	88	0.10	2.80	2.64	0.05		

Preparation of coagulants by base-titration

The 10 poly-aluminum chlorides (PACls) were produced by base-titration. These PACls are designated by the following rules: the number after "B" represents "% basicity", "s" indicates "sulfated", "ns" indicates "non-sulfate", "heat" indicates "heated", the number after "s" represents "mole ratio of sulfate ion to aluminum: SO_4/Al", and the number after the hyphen indicates serial number. $AlCl_3 \cdot 6H_2O$, $Al_2(SO_4)_3 \cdot 14{\sim}18H_2O$, and Na_2CO_3 were provided by FUJIFILM Wako Pure Chemical Corporation (Osaka, Japan), and NaOH was by Kanto Chemical Co., Inc., (Tokyo, Japan).

B65ns was prepared as follows: an $AlCl_3$ solution (0.5 M as Al, 80 mL) in a 500 mL Erlenmeyer flask was titrated with NaOH (0.24 M, 320 mL) by means of a peristaltic pump at a rate of 4 mL/min. During the titration, a combined hot plate/magnetic stirrer was used to agitate the solution in the flask and maintain the temperature at 85–90℃. B80ns-1 was prepared with the same materials and procedure for B65ns, except that the concentrations of $AlCl_3$ solution and NaOH were 0.25 M as Al and 0.15 M. The same materials and procedure were used to prepare B80ns-2, except that the concentration of $AlCl_3$ solution was 0.3 M. B82s0.11 was prepared as follows: an Al solution (0.49 M as Al, SO_4/Al=0.11 in mole ratio, 80 mL) was prepared with $AlCl_3$ and $Al_2(SO_4)_3$ in a 500 mL Erlenmeyer flask and titrated with NaOH (0.3 M, 320 mL) as the same procedure described above.

B65ns-heat was prepared by heating B65ns at 121℃ for 5 h with an autoclave (MLS-3781, PHC Holdings Corporation, Tokyo, Japan). B80ns-2-heat was prepared by heating B80ns-2 at 120℃ for 20 min with the same autoclave. B80s0.05-heat was prepared by heating B82s0.11 at 90~95℃ for 72 h with a combined hot plate/magnetic stirrer.

B79s0.10-1 was prepared by adding a Na_2CO_3 solution and an $Al_2(SO_4)_3$ solution into B65ns at ambient temperature until the basicity became 79% (calculation of the basicity is described in paragraph 2.2 of the main paper) and SO_4/Al became 0.10. B79s0.10-2-heat was prepared by adding a Na_2CO_3 solution and an $Al_2(SO_4)_3$ solution into B65ns-heat at ambient temperature. B88s0.10 was also prepared by adding a Na_2CO_3 solution and an $Al_2(SO_4)_3$ solution into B80ns-2 at ambient temperature.

Table 4S. The mixing conditions of coagulation in the jar-test (Figures 13S to 16S).

SPAC	Coagulant	Flash		Slow						Total
Median diameter	Dosage	G_F	T_F	G_{S1}	T_{S1}	G_{S2}	T_{S2}	G_{S3}	T_{S3}	G_TT_T
μm	mg-Al/L	s^{-1}	s	s^{-1}	s	s^{-1}	s	s^{-1}	s	dimensionless
1.0	0~1.5	190	60	19	600					22,800
1.0	0~1.5	200	60	20	600	15	600	10	1,200	45,000
1.1	1.5	200	120	20	600	15	600	10	1,200	57,000

Jar-tests using the coagulants made by base-titration

Filtered tap water was obtained by the method described in the main text of this paper (paragraph 2.3) except that its alkalinity was not adjusted. The water was supplemented with an SPAC slurry (median diameter is described in Table 4S) at concentration 10 mg/L to make raw water for the experiment consisting of coagulation-flocculation and sedimentation (jar test). Jar-tests were conducted in a 1-L rectangular beaker. After a predetermined volume of HCl or NaOH (0.1 N) was added to order to achieve the coagulation pH at 7.0, the coagulant (PACl) was injected into the beaker to a final concentration between 0 and 1.5 mg-Al/L (see also Table 4S). Then, the water was mixed rapidly and slowly. The mixing speed (G value) and times (T value) of the flash and slow mixing were varied depending on each experiment (see also Table 4S). The water was then left at rest for 1 h. A supernatant of 50 mL was sampled and determined for turbidity (2100Q portable turbidimeter; Hach Company, Loveland, CO, USA).

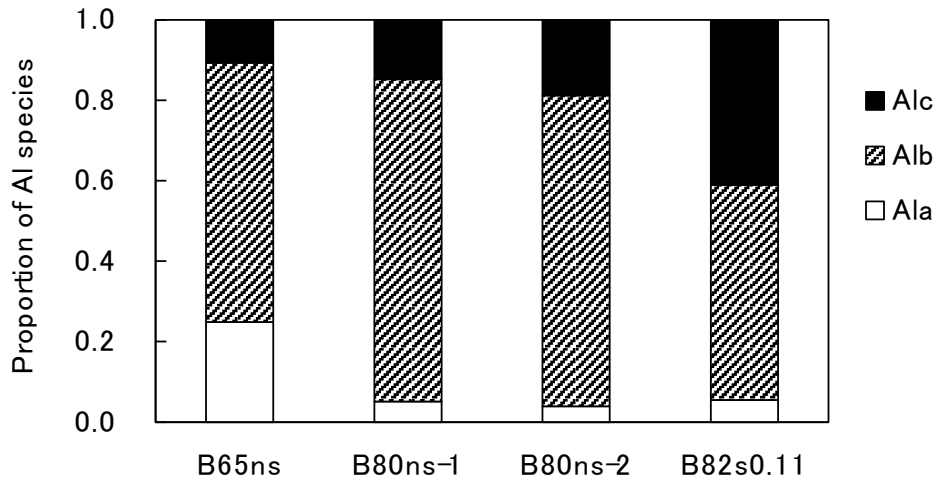

Figure 12S. Proportions of Al species in PACl coagulants made by base-titration.

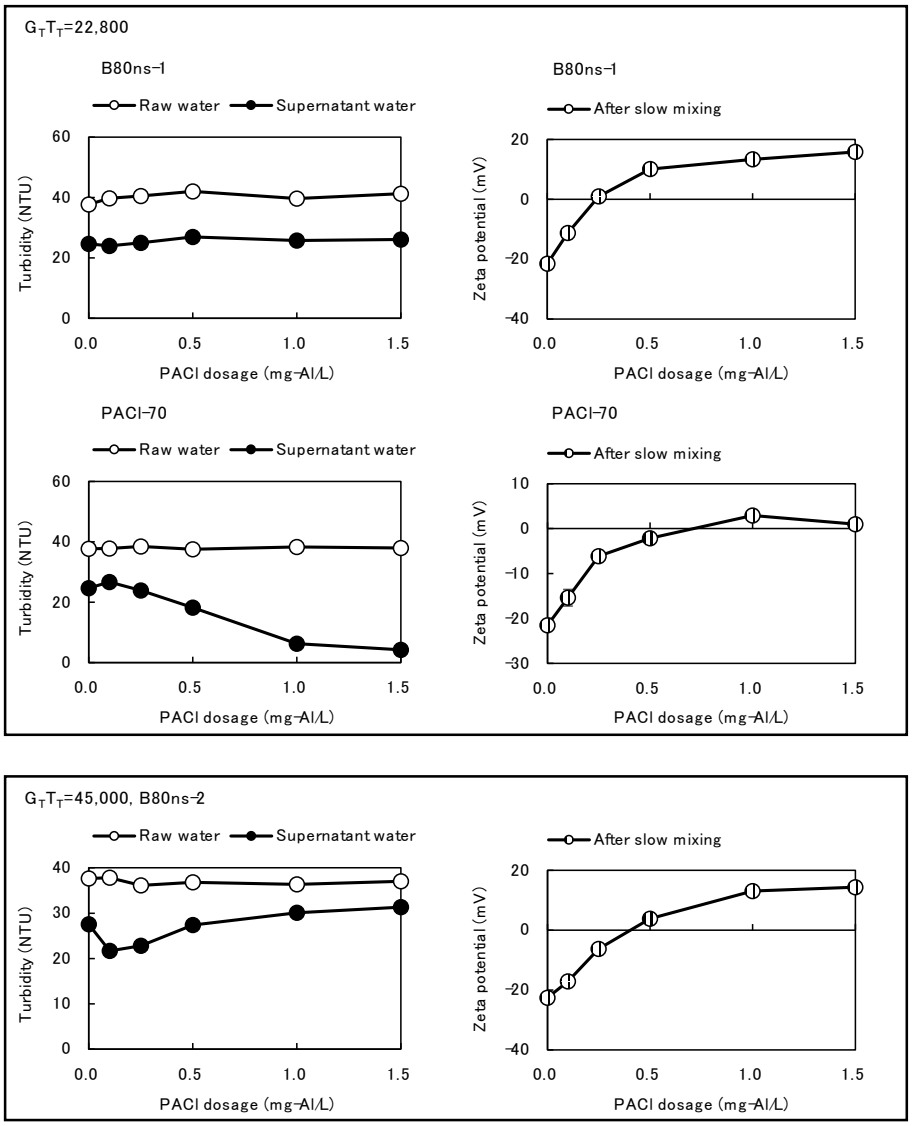

Figure 13S. Turbidity removal of and zeta potential of carbon particles. Initial SPAC concentration was 10 mg/L. Alb type base-titration PACls (B80ns-1, B80ns-2) and PACl-70 were used as coagulant with a dosage of 0 to 1.5 mg-Al/L. Coagulation pH was 7.0. Settling time was 60 min. Error bars of turbidity and zeta potential indicate standard deviations of three measurements and five measurements, respectively. Details of the mixing conditions are shown in Table 4S.

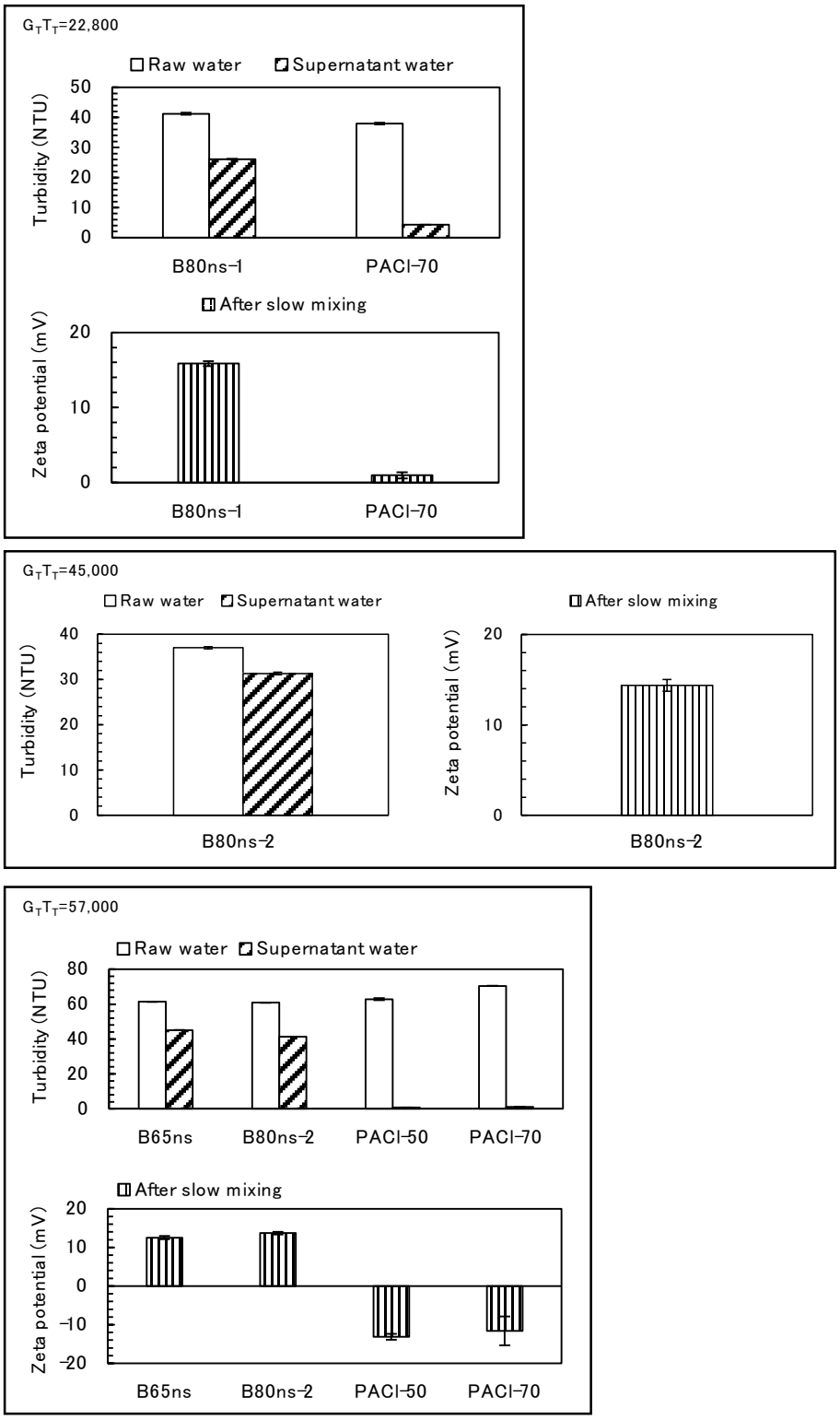

Figure 14S. Turbidity removal of and zeta potential of carbon particles. Initial SPAC concentration was 10 mg/L. Alb type base-titration PACls (B65ns, B80ns-1 and B80ns-2), PACl-50, and PACl-70 were used as coagulant with a dosage of 1.5 mg-Al/L. Coagulation pH was 7.0. Settling time was 60 min. Error bars of turbidity and zeta potential indicate standard deviations of three measurements and five measurements, respectively. Details of the mixing conditions are shown in Table 4S.

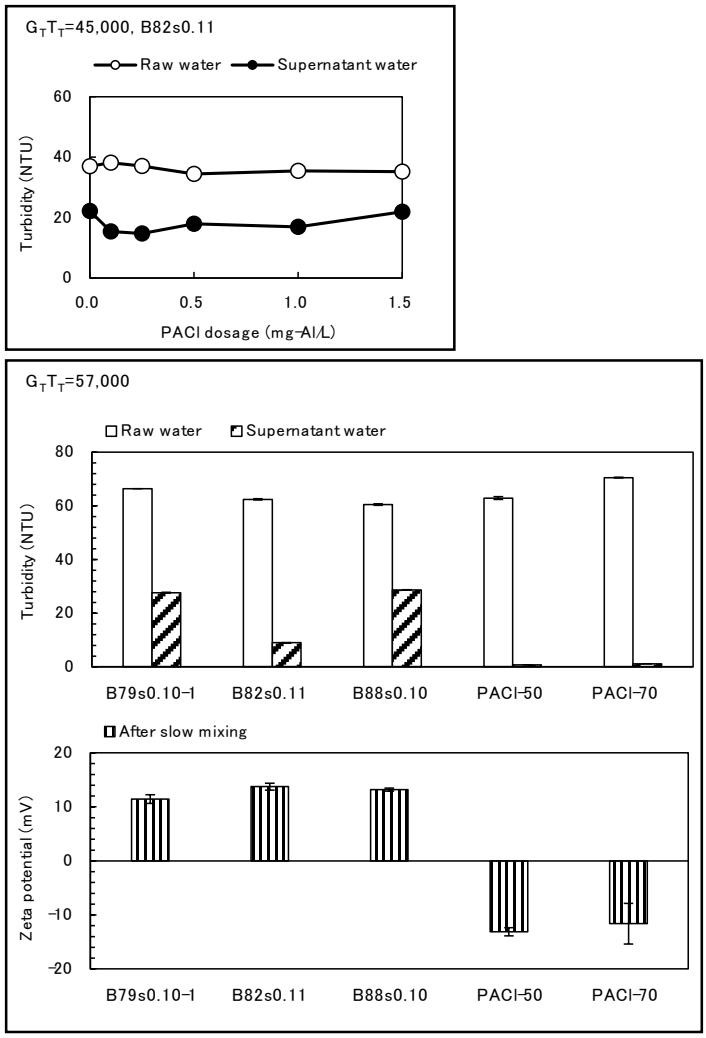

Figure 15S. Turbidity removal and zeta potential of carbon particles. Initial SPAC concentration was 10 mg/L. Base-titration PACls that contained sulfate ion (B79s0.10-1, B82s0.11, B88s0.10), PACl-50, and PACl-70 were used as coagulant with a dosage of 0 to 1.5 mg-Al/L. Coagulation pH was 7.0. Settling time was 60 min. Error bars of turbidity and zeta potential indicate standard deviations of three measurements and five measurements, respectively. Details of the mixing conditions are shown in Table 4S.

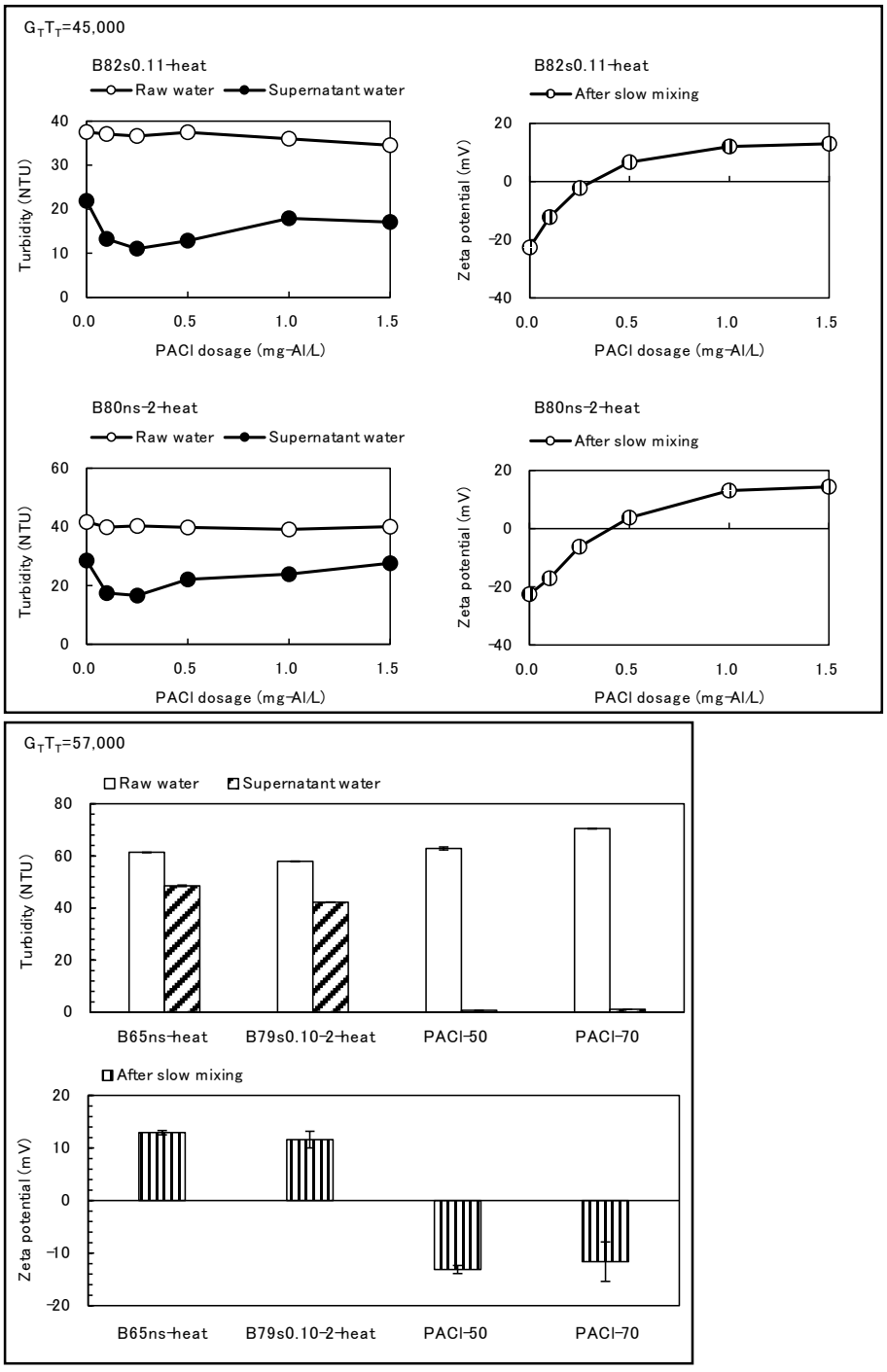

Figure 16S. Turbidity removal and zeta potential of carbon particles. Initial SPAC concentration was 10 mg/L. Alc-type base-titration PACls (B82s0.11-heat, B80ns-2-heat, B65ns-heat, and B79s0.10-2-heat), PACl-50, and PACl-70 were used as coagulant with a dosage of 0 to 1.5 mg-Al/L. Coagulation pH was 7.0. Settling time was 60 min. Error bars indicate standard deviations of measurements. Details of the mixing conditions are shown in Table 4S.

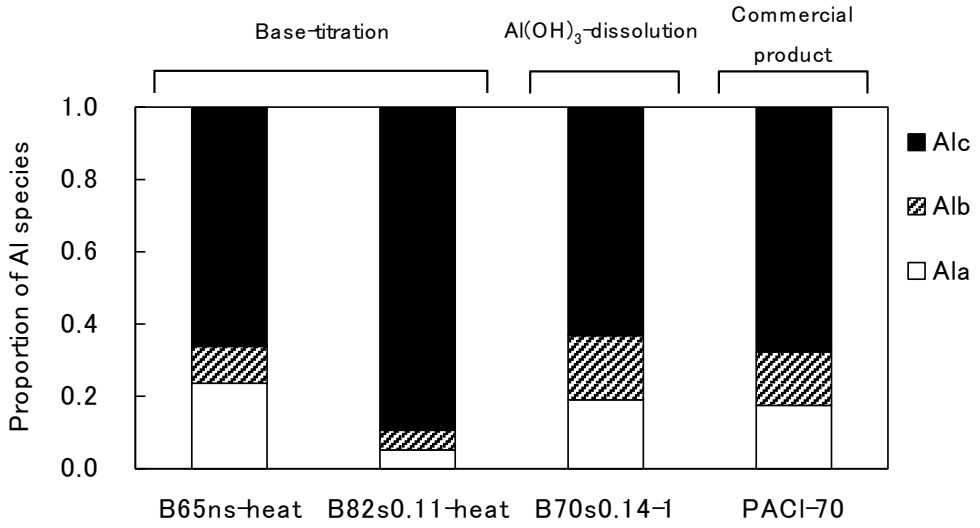

Figure 17S. Proportions of Al species in PACl coagulants made by base-titration, $Al(OH)_3$-dissolution, and commercial product.

Referene

Matsui, Y., Shirasaki, N., Yamaguchi, T., Kondo, K., Machida, K., Fukuura, T. and Matsushita, T. (2017) Characteristics and components of poly-aluminum chloride coagulants that enhance arsenate removal by coagulation: Detailed analysis of aluminum species. Water Research 118, 177-186.